A&A 450, 1037–1050 (2006)
DOI: 10.1051/0004-6361:20054626


Astronomy & Astrophysics

# Are $^{44}$Ti-producing supernovae exceptional?⋆

L.-S. The[1], D. D. Clayton[1], R. Diehl[2], D. H. Hartmann[1], A. F. Iyudin[2,3], M. D. Leising[1], B. S. Meyer[1], Y. Motizuki[4], and V. Schönfelder[2]

[1] Department of Physics and Astronomy, Clemson University, Clemson, SC 29634-0978, USA
e-mail: tlihsin@clemson.edu
[2] Max-Planck-Institut für Extraterrestrische Physik, Postfach 1312, 85741 Garching, Germany
[3] Skobeltsyn Institute of Nuclear Physics, Moscow State University, Vorob'evy Gory, 119992 Moscow, Russia
[4] Cyclotron Center, RIKEN, Hirosawa 2-1, Wako 351-0198, Japan

Received 1 December 2005 / Accepted 15 December 2005

**ABSTRACT**

According to standard models supernovae produce radioactive $^{44}$Ti, which should be visible in gamma-rays following decay to $^{44}$Ca for a few centuries. $^{44}$Ti production is believed to be the source of cosmic $^{44}$Ca, whose abundance is well established. Yet, gamma-ray telescopes have not seen the expected young remnants of core collapse events. The $^{44}$Ti mean life of $\tau \simeq 89$ y and the Galactic supernova rate of $\simeq$3/100 y imply $\simeq$several detectable $^{44}$Ti gamma-ray sources, but only one is clearly seen, the 340-year-old Cas A *SNR*. Furthermore, supernovae which produce much $^{44}$Ti are expected to occur primarily in the inner part of the Galaxy, where young massive stars are most abundant. Because the Galaxy is transparent to gamma-rays, this should be the dominant location of expected gamma-ray sources. Yet the Cas A *SNR* as the only one source is located far from the inner Galaxy (at longitude 112°). We evaluate the surprising absence of detectable supernovae from the past three centuries. We discuss whether our understanding of SN explosions, their $^{44}$Ti yields, their spatial distributions, and statistical arguments can be stretched so that this apparent disagreement may be accommodated within reasonable expectations, or if we have to revise some or all of the above aspects to bring expectations in agreement with the observations. We conclude that either core collapse supernovae have been improbably rare in the Galaxy during the past few centuries, or $^{44}$Ti-producing supernovae are atypical supernovae. We also present a new argument based on $^{44}$Ca/$^{40}$Ca ratios in mainstream SiC stardust grains that may cast doubt on massive-He-cap type I supernovae as the source of most galactic $^{44}$Ca.

**Key words.** ISM: abundances – Galaxy: abundances – gamma rays: observations – ISM: supernova remnants – supernovae: general – dust, extinction

## 1. Introduction

Supernovae are the agents that drive the evolution of gaseous regions of galaxies. As end points of the evolution of massive stars that have formed out of the interstellar gas, their explosions eject matter enriched with freshly formed isotopes and stir interstellar gas. However, the explosions themselves are still not understood (Burrows 2000; Janka et al. 2003). Parametric descriptions are used to describe the core collapses ("cc-SN", supernovae of types II and Ib/c) (Woosley & Weaver 1995; Thielemann et al. 1996) as well as thermonuclear explosions of white dwarfs (supernovae of type Ia; Nomoto et al. 1997). A prominent issue in astrophysics is whether the supernova explosion itself is a well-regulated, robust physical process, or if intrinsic variability over a wider range of physical conditions are rather common.

Supernova homogeneity by type can be studied in different ways. One approach is to analyze the rate of supernovae of a specific type in different environments and over different time scales. In this work we do this by asking if the current rate of supernovae in our Galaxy which produce radioactive $^{44}$Ti is in line with expectations from other observables and from supernova theory.

$^{44}$Ti decay offers a unique window to the study of supernova rates. Specific aspects of this window are:

1. Gamma rays penetrate the entire galactic disk with little extinction.
2. $^{44}$Ti gamma-rays reflect the current rate of supernovae, with the $^{44}$Ti mean decay time scale of $\tau = 89$ years; this present-day snapshot which has not yet fed back into chemical evolution can be directly related to the observable current population of massive stars.
3. Most $^{44}$Ti is co-produced with $^{56}$Ni in relatively frequent core collapse supernovae (cc-SN). The radioactive energy of $^{56}$Ni is responsible for well-observed supernova light.

⋆ Appendices are only available in electronic form at http://www.edpsciences.org

4. Nucleosynthesis of $^{44}$Ti is primarily from $\alpha$-rich freeze-out of nuclear statistical equilibrium and secondarily from silicon burning.
5. The origin of abundant cosmic $^{44}$Ca occurs mainly through $^{44}$Ti nucleosynthesis.
6. $^{44}$Ti traces have been found in pre-solar grains which have been attributed to condensation within core-collapse supernovae.

In this paper we estimate what the gamma-ray sky of $^{44}$Ti sources would be expected to look like by adopting an *average $^{44}$Ti source model* having a characteristic source event *recurrence rate, $^{44}$Ti yield per event*, and *spatial distribution*. We compare this to the present-day gamma-ray survey and find apparent and serious conflicts. Then we analyze whether deviations from these *average* expectations can occur from the known or expected *variability of models and parameters involved*. We use a Monte Carlo simulation of the expected sky image within reasonable distributions of parameters for that purpose. This leads us to discuss each of the relevant parameters, which may explain an anomalous $^{44}$Ti sky; these are, specifically:

– the gamma-ray survey quality;
– statistical effects of small samples;
– the adopted supernova rates;
– the supernova explosion and nucleosynthesis models;
– the spatial distribution of supernova events;
– the deviations from smooth chemical evolution;
– the supernova origin of Galactic and solar $^{44}$Ca.

## 2. $^{44}$Ti and supernovae in the Galaxy

Supernova rates in the Galaxy can be inferred from different observables. But observational incompleteness and bias requires that several assumptions are an essential part of such inferences. We compare here the observed $^{44}$Ti sky with expectations for the occurrences of young $^{44}$Ti emitting supernova remnants, as they result from astrophysical assessments of supernova characteristics for our Galaxy. We choose a time interval unit of 100 years for comparison of chemical history with supernova event rates. The extrapolation of the past history and yields of $^{44}$Ti-ejecting supernova events should give a production rate which can be compared with recent supernova rates, as no other source of $^{44}$Ca has yet been identified.

Have the $^{44}$Ca-producing supernovae been typical; is all of $^{44}$Ca produced through radioactive $^{44}$Ti; or do exceptional events contribute most of the $^{44}$Ti? Gamma-ray surveys for $^{44}$Ti sources, and presolar supernova grains provide ways to address this question.

In the following section we will then examine each of the critical assumptions in more detail.

For a $^{44}$Ti sky reference, we adopt the result from COMPTEL's survey in the 1.157 MeV band, which is the most complete survey to date (Dupraz et al. 1997; Iyudin et al. 1999). In this survey, one object has been clearly detected (340-year-old Cas A at a distance of 3.4 kpc), candidates at lower significance have been discussed (most prominently GRO J0852-4642 in the Vela region, Iyudin et al. 1999), and a weak signal from the Per OB2 association (Dupraz et al. 1997). Apparently, no bright young $^{44}$Ti emitting supernova remnants are found in the inner region of the Galaxy (see Fig. 1).

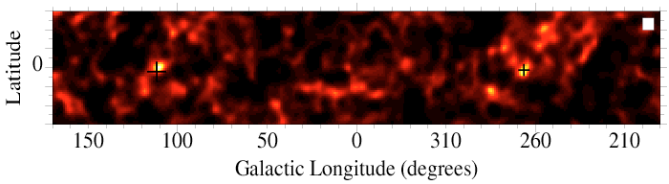


**Fig. 1.** Maximum-entropy map of the Galactic plane (within latitude ±30°) in the $^{44}$Ti energy window (1.066–1.246 MeV) for the combination of CGRO observations from 0.1 to 617.1. Two crosses mark the positions of Cas A and GRO J0852-4642. This figure is adopted from Iyudin (1999).

What do we expect the Galaxy to look like in $^{44}$Ti emission?

### 2.1. $^{44}$Ti from supernovae

*Supernova observations* directly demonstrate that these events are at the origin of $^{44}$Ti production: the 1.157 MeV $\gamma$-ray line following $^{44}$Ti decay has been detected in the 340-year old Galactic supernova remnant Cas A (Iyudin et al. 1994; Vink et al. 2001). Furthermore, SN1987A's late light curve, observed in unique detail over more than 15 years, appears powered by a similar amount of $^{44}$Ti ($0.2–2.0 \times 10^{-4}$ $M_\odot$), from modeling of radioactive energy deposition and photon transport in the *SNR* (Woosley et al. 1989; Fransson & Kozma 2002). Gamma-ray detection and proof of this interpretation is still lacking, but INTEGRAL's recent observations may prove sufficiently sensitive.

*Presolar grains* have been identified in meteoritic samples through their unusual isotopic abundance patterns, and hold rich isotopic abundance detail for characterizing their condensation environments (e.g. Clayton & Nittler 2004; Zinner 1998). SiC grains of the X-type are attributed to core-collapse supernovae from their large excesses in characteristic isotopes (Nittler et al. 1996). $^{44}$Ti-produced overabundance of $^{44}$Ca is found in these SiC X grains, indicating presence of $^{44}$Ti at their time of condensation. Measured $^{44}$Ca/$^{40}$Ca ratios are large (Nittler et al. 1996; Clayton et al. 1997a; Hoppe et al. 2000). This proves their supernova origin, on one hand, and likewise it proves that dust-producing supernovae may eject $^{44}$Ti in significant amounts. Their attribution to core collapse supernovae rather than supernovae of type Ia (Nittler et al. 1996) is plausible, if we believe that core collapse supernovae probably dominate $^{44}$Ti production and because there is no direct evidence of dust condensation in thermonuclear supernovae (Dwek 1998). It is likely that all of the observed X grains sample both different condensation environments and different production events. Therefore, their $^{44}$Ca abundances cannot be interpreted in absolute terms as a measure of the mass of $^{44}$Ti ejected per supernova.

*The most plausible cosmic environment for production of $^{44}$Ti* is the $\alpha$-rich freeze-out from high-temperature burning near Nuclear Statistical Equilibrium (e.g. Woosley et al. 1973;

Arnett 1996). The required high values for the entropy are found in core-collapse supernovae. Therefore the simplest plausible assumption is that core-collapse supernovae are responsible for any substantial sources of $^{44}$Ti.

It is likewise plausible that traditional SNIa do not add significantly to nucleosynthesis at mass $A = 44$, specifically no $^{44}$Ti, since their NSE freeze-out conditions will not be favorable for $^{44}$Ti production (Timmes et al. 1995). We consider the symbiotic-star scenario as a rare subclass of SNIa, even though their $^{44}$Ti yields may be large (Woosley & Weaver 1994); so they indeed would be rare outliers, rather than typical $^{44}$Ti producing supernovae. We will discuss uncertainties in each of these sites in more detail below (see Sect. 3.5).

### 2.2. Ca from supernovae

Measurements of *cosmic isotopic abundances* can be converted into isotope production rates; however, for all long-lived isotopes models of chemical evolution have to be applied (e.g. Clayton 1988; Pagel 1997; Timmes et al. 1995; Matteucci 2003). How can we use these for predicting the shortlived $^{44}$Ti source appearance in gamma-rays? Its lifetime is too short for mean chemical evolution arguments.

Over the time scale of chemical evolution of the Galaxy, the cumulative and averaging effects of different explosion types would integrate to a smooth pattern of "standard abundances", as they are observed throughout the universe. Evolutionary pathways for individual elements can be associated with the evolution of metallicity and the rates of different supernova types. The abundance of $^{44}$Ca in solar-system matter thus can be translated through models of chemical evolution into a current average production rate of $\simeq 3 \times 10^{-4}\ M_\odot$ of $^{44}$Ti per 100 y (Leising & Share 1990, see below).

Chemical evolution calculations (Timmes et al. 1995) using computed ejecta masses (Woosley & Weaver 1995) were shown to account reasonably for most solar abundances, including specifically $^{40}$Ca, but failing by a factor of three for $^{44}$Ca; this fact is also evident from the ratio of $^{44}$Ti to Fe in cc-SN models. But over short time scales where only a limited number of source events contribute, great variability among sources would present a significant difference of the present-day picture from the average. Therefore we may compare the expectations from long-term averaged $^{44}$Ti production to the present-day $^{44}$Ti source record imaged in gamma-rays, allowing for the short-term fluctuations with Monte-Carlo realizations of the sources.

*The solar-system $^{44}$Ca abundance* is rooted plausibly in $^{44}$Ti nucleosynthesis (Woosley et al. 1973; Clayton 1982), and is a result of the integrated Galactic nucleosynthesis prior to formation of the solar system. Given a time-dependence of the production rate, it can be normalized to the rate required to give precisely the measured solar abundance 4.5 Gyr ago, which also fixes the long-term average production rate today. Models of galactic chemical evolution, constrained by a number of observables, provide us with that time dependence, albeit subject to a number of assumptions and parameter choices. Adjusting the $^{44}$Ti yield in the aforementioned calculation (Timmes et al. 1995) upward by a factor of three to achieve the solar abundance, we infer a production rate of $^{44}$Ca of about $3.6 \times 10^{-6}\ M_\odot\ \mathrm{yr}^{-1}$. Other considerations using different chemical evolution models (see Appendix C) lead from the $^{44}$Ca abundance to a current $^{44}$Ti production rate: $p(^{44}\mathrm{Ti}) = 5.5 \times 10^{-6}\ M_\odot\ \mathrm{yr}^{-1}$, with full uncertainty range $1.2\text{–}12 \times 10^{-6}\ M_\odot\ \mathrm{yr}^{-1}$ (see Appendix C).

### 2.3. Supernova rates

Direct supernova rate measures have been made through correlations between supernova activity and other tracers of the massive star content of a galaxy. van den Bergh (1991) finds $(2.62 \pm 0.8)\ h_{100}^2$ SN century$^{-1}$. For $h_{100} = 0.75$, the rate is $1.5 \pm 0.8$ SN century$^{-1}$. This rate is based on a combined study of galactic supernova remnants, historical SNe, and novae in M 31 and M 33. Cappellaro et al. (1993) refer to this rate as the best estimate. van den Bergh & Tammann (1991) find $SNR = 4.0$ SN century$^{-1}$. The authors review supernova rates in external galaxies and derive a specific supernova frequency, in units of 1 SNu = one SN per century per $10^{10}\ L_\odot$(B), for various galaxy types. If one assumes that the Galaxy is intermediate between types Sab-Sb and types Sbc-Sd, the specific rate is $3\ h_{100}^2$ SNu. For a Galactic blue-band luminosity of $L(\mathrm{B}) = 2.3 \times 10^{10}\ L_\odot(\mathrm{B})$ (their Table 11) and $h_{100} = 0.75$ we infer $SNR = 4.0$ SN century$^{-1}$. Their review paper also discusses estimates from internal tracers in the Milky Way: from radio supernova remnant (RSNR) statistics they infer $SNR = 3.3 \pm 2.0$ SN century$^{-1}$. From the historic record of nearby (<a few kpc) supernovae in the past millennium they find $SNR = 5.8 \pm 2.4$ SN century$^{-1}$. The large extinction corrections in the galactic plane make this small sample highly incomplete, which results in large uncertainties in extrapolations to the full galactic disk. The authors also review efforts based on the pulsar birth rate, but extensive observational selection effects in combination with the strong and poorly understood evolution of luminosity and beaming geometry (see Lyne & Graham-Smith 1998; and Lorimer & Kramer 2004) renders this method impractical for estimating the galactic SNR. Continuing the studies of van den Bergh & Tammann, Cappellaro et al. (1993) find $SNR = 1.4 \pm 0.9$ SN century$^{-1}$, when scaling to external galaxies of similar type. The sample is obtained from surveys carried out at the Asiago and Sternberg Observatories. The authors provide an extensive discussion of the uncertainties of this method, which can exceed 200% for some late type galaxies. More recently, van den Bergh & McClure (1994) find $SNR = (2.4\text{–}2.7)\ h_{75}^2$ events per century. This estimate is based on re-evaluation of the extra-galactic SN rates obtained from Evans' 1980–1988 observations. This method depends on a somewhat uncertain type of the Galaxy and the value of its blue-band luminosity, while the uncertainty due to the Hubble constant is now very small. Given the error analysis in the paper, the rate is uncertain by at least 30%.

van den Bergh & McClure (1994) in studying the supernova rates of local spiral galaxies of types Sab-Sd of Evans' observations estimated that 80%–90% of supernova in that galaxies are of types Ibc and II. Recently Cappellaro (2003) combining five

SN searches to include 137 SNe in 9346 galaxies estimates the SN type ratios in the Galaxy to be Ia:Ib/c:II = 0.22:0.11:0.67. From these observations, one infers a ratio of core-collapse to thermonuclear supernova of $R$ = (II+Ibc)/Ia = 3.5. However, note that the Galactic historical record in the last millennium shown in Table B.1 contains only two type Ia *SNR* out of six *SNR*s. An often used alternative distribution over types is Ia:Ib/c:II = 0.1:0.15:0.75 (Hatano et al. 1997; Dawson & Johnson 1994; Tammann et al. 1994; Hartmann et al. 1993), which implies a three times higher cc-SN fraction. In this work, we adopt this set of parameters, and note that the small $^{44}$Ti yield of type Ia renders our results insensitive to this ratio.

Over the last millennium, the historic record contains six events (see Appendix B.4), which implies a rather low rate at face value. However Galactic extinction at visible wavelengths and embedded supernovae will lead to large occultation bias, and with extinction models plus Monte Carlo simulations this historic record can be assessed to approximately agree with extragalactic rate determinations (see Sect. 3 and Appendix A.2). An often cited rate of galactic cc-SN of three per century is consistent both with astronomical arguments (van den Bergh & McClure 1990) and with the rate inferred by Timmes et al. (1995) from their chemical evolution model that produces solar abundances successfully. We adopt a supernova recurrence rate of 30 years as a baseline for our $^{44}$Ti sky expectations.

### 2.4. Supernova locations

The 1.157 MeV $\gamma$-ray line following $^{44}$Ti decay has been detected in the 340-year old Galactic supernova remnant Cas A (Iyudin et al. 1994; Vink et al. 2001). COMPTEL's survey (Dupraz et al. 1997; Iyudin et al. 1999) has resulted in other candidate sources, such as the so-called Vela junior *SNR* (Iyudin et al. 1998). INTEGRAL's inner-Galaxy survey has been studied with IBIS Imager data, which did not reveal a new source in this region (Renaud et al. 2004). The difficulties of MeV observations have thus not led to convincing new $^{44}$Ti rich supernova remnants, especially in the inner Galaxy region ($l = 0° \pm 30°$) where observations are deepest. Yet, Cas A seems an established $^{44}$Ti detection in COMPTEL (Schönfelder et al. 2000) and Beppo-Sax (Vink et al. 2001) and INTEGRAL/IBIS (Vink 2005) measurements, while OSSE (The et al. 1996) and RXTE (Rothschild & Lingenfelter 2003) measurements of Cas A were not sufficiently sensitive. There exist no well-understood supernova remnants other than Cas A where the $^{44}$Ti production issue can be tested. It is apparently the only supernova whose yield, age, and nearness makes $^{44}$Ti visible in gammas. Naturally we ask ourselves if Cas A is a typical supernova or an anomalous case of a high-$^{44}$Ti yield supernova?

Current supernova models predict an amount of $^{44}$Ti which is of the same order than what these observations suggest, though generally slightly less. Can we take this as a satisfactory confirmation of our understanding of core collapse supernova $^{44}$Ti production? These two identified core collapse events and their association with $^{44}$Ti production appear to be in line with models which attribute $^{44}$Ti production to the more frequent standard core collapse events but not to standard thermonuclear supernovae. Is this correct?

If true, the location of $^{44}$Ti sources should match the locations of young massive stars which have rather short lifetimes. There is substantial evidence that massive star formation occurs in spiral arms and predominantly in the inner Galaxy (Elmegreen et al. 2003; Scoville et al. 2001; Kennicutt 1998). Massive stars can be observed directly in the infrared (e.g. Maeder & Conti 1994), though extinction corrections are large in regions of dense clouds. Possibly an even better (though more indirect) massive-star census can be derived from $^{26}$Al decay $\gamma$-rays (Diehl et al. 1995; Prantzos & Diehl 1996; Knödlseder 2000; Diehl et al. 2005). $^{26}$Al is understood to originate predominantly from massive stars and $\gamma$-rays easily penetrate even dark clouds in star forming regions. So, do we see the $^{44}$Ti sources in regions where we expect them to occur? Or do other factors which are not yet understood conspire to make $^{44}$Ti ejection a phenomenon of core collapse events occurring in special regions and environments?

### 2.5. Estimating the $^{44}$Ti sky appearance

If we want to estimate how the $^{44}$Ti sky should appear in a gamma-ray survey, we need to follow a statistical approach, due to the rare occurrence of supernovae. We therefore apply a Monte Carlo approach of sampling plausible probability distributions for supernova rates, their $^{44}$Ti yields, and their Galactic distribution, thus calculating a large statistical sample of possible appearances of the $^{44}$Ti sky.

- The mean rate of supernovae in our Galaxy is taken as one event in 30 years.
- $^{44}$Ti producing supernova events can be of type Ia, Ib/c, or II SNe. For this study, we choose a supernova type ratio, Ia:Ib/c:II = 0.10:0.15:0.75 (Dawson & Johnson 1994; Hatano et al. 1997).
- Supernovae are then assumed to produce $^{44}$Ti according to models of that type. In our models, type II supernova yields are generated according to stellar mass, which is drawn from a Salpeter-type initial mass distribution for $M \geq 8\ M_\odot$; the $^{44}$Ti yields per mass of the star are taken from Table 1 of Timmes et al. (1996). A typical yield is $3 \times 10^{-5}\ M_\odot$ for $M = 25\ M_\odot$, but variations with mass are about a factor 2. The $^{44}$Ti yields of type Ib SNe are uniformly distributed between $3 \times 10^{-5}\ M_\odot$ and $9 \times 10^{-5}\ M_\odot$ with typical values of $6 \times 10^{-5}\ M_\odot$ (Timmes et al. 1996). The $^{44}$Ti yields of type Ia SNe are uniformly distributed between $8.7 \times 10^{-6}\ M_\odot$ and $2.7 \times 10^{-5}\ M_\odot$ so this range covers the $^{44}$Ti yield in the deflagration W7 model, the delayed detonation WDD2 model, and the late detonation W7DT model of Nomoto et al. (1997). But instead of adopting the $^{44}$Ti ejecta masses directly from these models, we uniformly increase these by a factor 3 in order that chemical evolution calculations reproduce the known solar $^{44}$Ca/$^{40}$Ca ratio. This assumes that $^{44}$Ti and $^{44}$Ca nucleosynthesis are directly related and that some unknown physics factor causes the computed $^{44}$Ti masses to be uniformly low

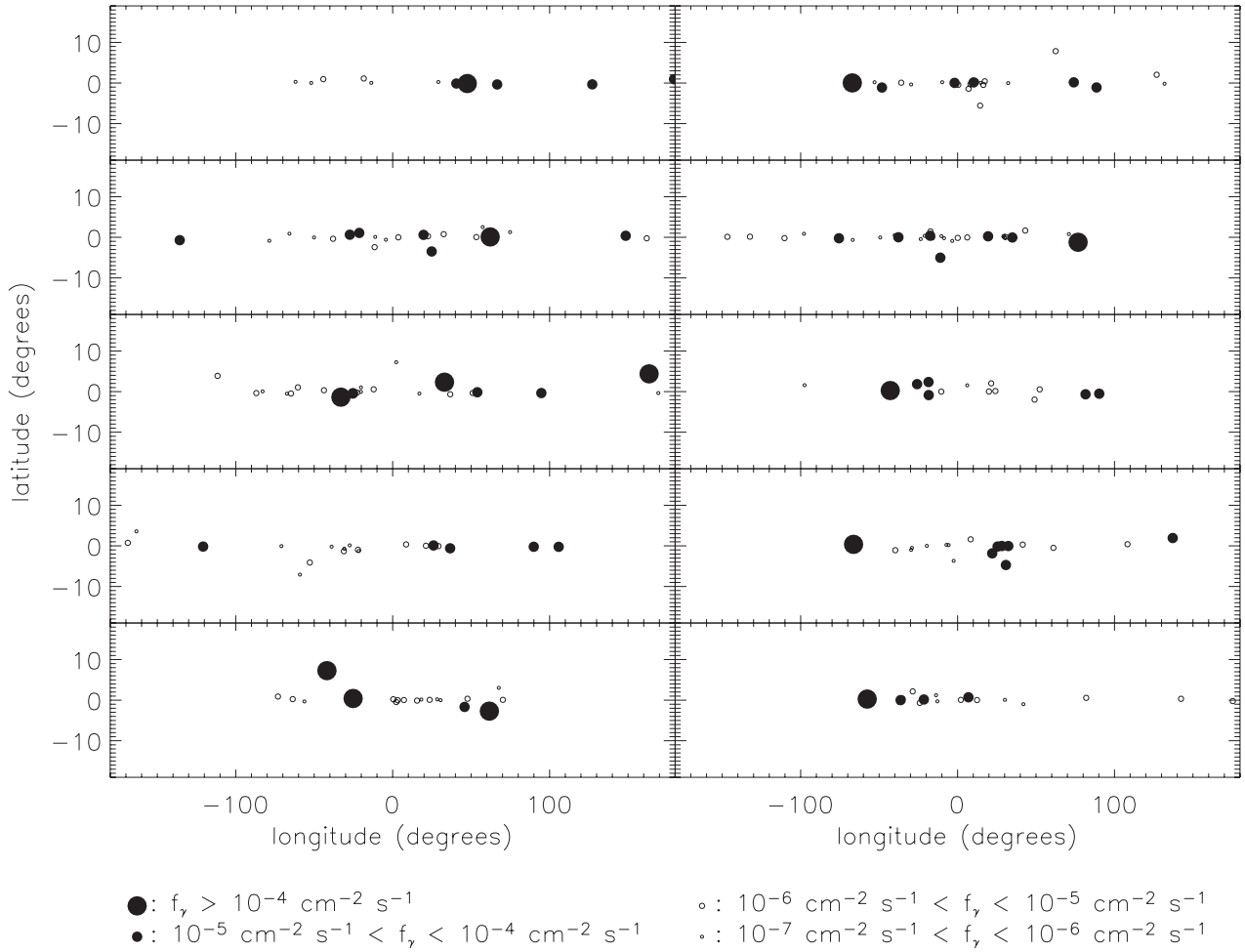


**Fig. 2.** The expected Ti sky of 10 simulated galaxies of model **A** where the supernova recurrence time is taken to be 30 years and the supernovae ratio of Ia:Ib:II = 0.10:0.15:0.75. Simulating a $10^5$ galaxy sky, a gamma-ray detector with a detection limit of $10^{-5}$ cm$^{-2}$ s$^{-1}$ would have a probability of detecting 0, 1, and 2 $^{44}$Ti sources of 0.0017, 0.012, and 0.037, respectively. A slightly better instrument than the $10^{-5}$ cm$^{-2}$ s$^{-1}$ detection limit would detect several $^{44}$Ti sources.

by a factor three. Note that $^{44}$Ti yields and supernova rate determine the brightness scale of our $^{44}$Ti sky expectations.

– For each supernova type, we then adopt a parent spatial distribution, from which we draw random samples to determine the location of the event. The spatial distribution for core-collapse supernovae (types Ib/c and II) is taken, from either an exponential disk with scale radii between 3.5 and 5 kpc, or from a Gaussian-shaped ring at 3.7 kpc radius with a thickness of 1.3 kpc, both placing young stars in the inner region of the Galaxy as suggested by many observables. Thermonuclear supernovae (type Ia) are assumed to arise from an old stellar population, hence we adopt the distribution of novae as our parent Galactic distribution for those rare events. We adopt the composite disk-spheroid nova model from Higdon & Fowler (1987) (see Appendix A for more detail on the variety of modeled distributions).
– We then randomly choose the individual supernova age within the last millennium, for deriving its $^{44}$Ti decay gamma-ray brightness. This assumes that the factors governing the mean recurrence rate have not changed in the past $10^3$ yr.

Randomly selected sample results from $10^5$ such realizations of an expected $^{44}$Ti sky are shown in Fig. 2, to be compared with the observed 1.157 MeV COMPTEL image shown in Fig. 1 (Iyudin et al. 1999). We illustrate how typical these expected images would be, by showing the distribution of source brightnesses over a much larger number of Monte Carlo samples (Fig. 3, left): a $^{44}$Ti flux above a representative limit of $10^{-5}$ ph cm$^{-2}$ s$^{-1}$ occurs in 19% of our $^{44}$Ti gamma-line flux distribution. The expected number of $^{44}$Ti point sources per galaxy lies above the gamma-ray survey sensitivity limit, i.e., we do expect typically 5–6 positive detections of $^{44}$Ti sources (see Fig. 3 right).

It is immediately evident from Figs. 2 and 3 that expectations based on such seemingly plausible assumptions look very different than the observed $^{44}$Ti sky: Fig. 2 shows ∼4–7 observable $^{44}$Ti sources in an area of the Galaxy that contained none (see Fig. 1) above the observable flux limit used for comparison. The brightest source in that realization (large-filled circles) has $I_\gamma \sim 10^{-4}$ cm$^{-2}$ s$^{-1}$, which would have been seen as a $\sim 10\,\sigma$ source by COMPTEL, and would have been detected already in INTEGRAL's inner-Galaxy survey (Vink 2004). The majority of our calculated samples lead to this same type of conflict (see

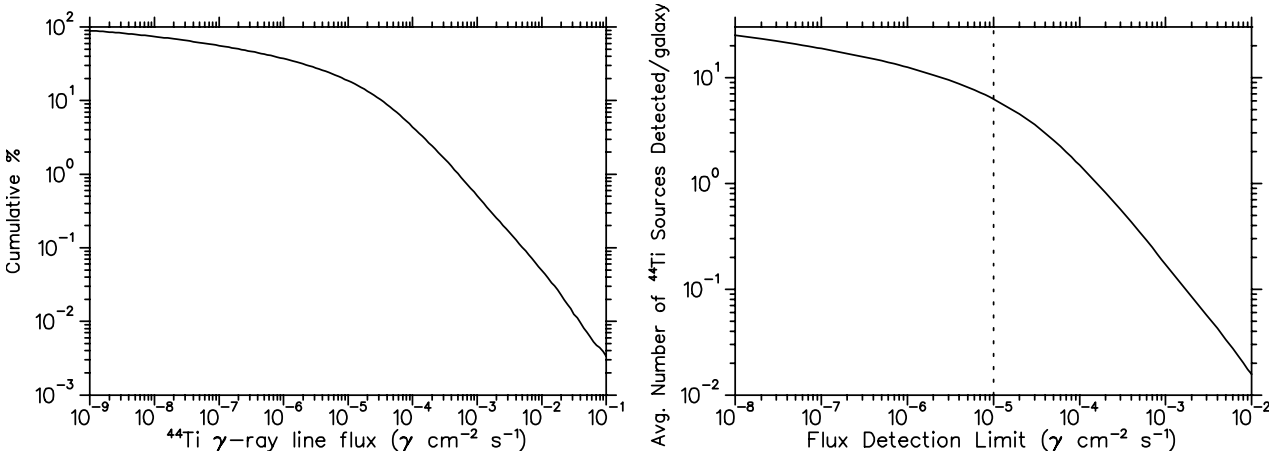


**Fig. 3.** Cumulative $^{44}$Ti gamma-ray line flux distribution of supernovae with $f_\gamma > 1\times10^{-12}$ cm$^{-2}$ s$^{-1}$ according to our Model **A** (see Appendix A.2) with supernovae type ratio of Ia:Ib:II = 0.1:0.15:0.75 (*left*). Expected average number of supernovae per sample galaxy with their $^{44}$Ti gamma-line fluxes above detection limits, for a supernova recurrence time of 30 yr, irrespective of their position in the sky (*right*). The detection limit of COMPTEL instrument is shown as a dotted line.

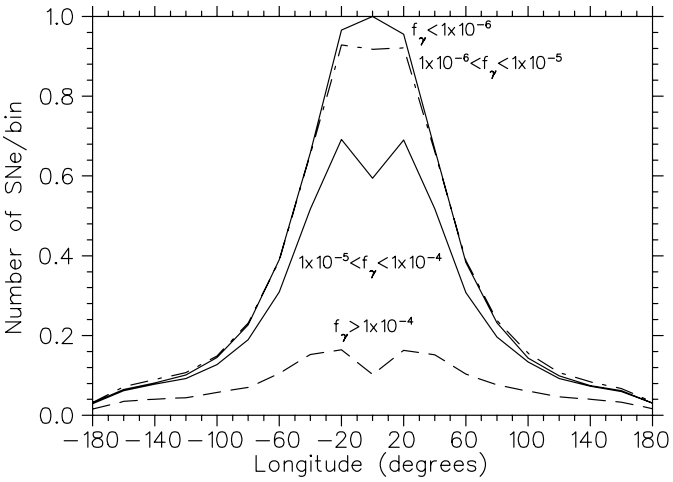


**Fig. 4.** The longitude distribution of supernovae for four $^{44}$Ti gamma-ray line flux bandwidths in Model **A** of Appendix A.2 with supernovae type ratio of Ia:Ib:II = 0.1:0.15:0.75. The equal-bin width is 20 degrees in longitude. Only the $f_\gamma < 1\times10^{-6}$ cm$^{-2}$ s$^{-1}$ distribution is normalized and multiplied by a factor of 0.298.

Fig. 3). The probability of having no sources within the central galaxy is small for current surveys, as illustrated in Fig. 4 (for model A): for a survey down to $I_\gamma \sim 10^{-5}$ cm$^{-2}$ s$^{-1}$, ~12% of supernovae appear within longitudes 0±60°, whereas only 72% of supernovae is within that volume. An interesting feature, however, is that the longitude distribution for $f_\gamma < 1\times10^{-5}$ cm$^{-2}$ s$^{-1}$ is dominated by sources from type Ia (the bulge) and farther away SNe, while the distribution for $f_\gamma > 1\times10^{-5}$ cm$^{-2}$ s$^{-1}$ is dominated by sources from type Ib and type II (disk) and nearby SNe. This feature also can be seen in Fig. 3, where around $f_\gamma \simeq 1\times10^{-5}$ cm$^{-2}$ s$^{-1}$ the distribution changes its slope.

It is clear that something is wrong with at least one of these assumptions:

- the rate of core collapse supernovae in the Galaxy is 3/100 y;
- a core collapse supernova produces $\simeq 10^{-4}$ $M_\odot$ of $^{44}$Ti;
- supernovae of each given type sample a relatively narrow range of the $^{44}$Ti yield, i.e., we do not consider extreme outliers event (nor do we consider a rare but superhigh yield source class);
- the locations of core collapse supernovae is axisymmetric i.e., we assume star formation in spiral arms is not dominant.

In the following we examine these questions, and seek possible explanations for the apparent conflict.

## 3. Resolving the $^{44}$Ti sky conflict

### 3.1. Gamma-ray observations

The $^{44}$Ti gamma-ray sky can be studied in lines from the primary decay to $^{44}$Sc at 67.9 and 78.4 keV and from the following decay to $^{44}$Ca at 1.157 MeV. In this latter line, the COMPTEL imaging telescope had reported the pioneering detection of $^{44}$Ti from Cas A (Iyudin et al. 1994), clearly showing a point source image at 1.157 MeV as well as the line in a spectrum from this source. This detection had initially created some controversy because other gamma-ray instruments apparently did not see it (The et al. 1996; Rothschild et al. 1998). We now believe that this is due to the high initially-reported COMPTEL gamma-ray flux value, reduced later with better statistical accuracy of the measurement (Iyudin et al. 1999; Dupraz et al. 1997). The independent detections with BeppoSax (Vink et al. 2001) and with INTEGRAL/IBIS (Vink 2005) in both lower-energy lines (Beppo-SAX) and in the 67.9 keV line (IBIS) now consolidate the $^{44}$Ti detection from Cas A, but also suggest that indeed the $^{44}$Ti gamma-ray flux of Cas A is in a range between 0.8 and $3.5\times10^{-5}$ ph cm$^{-2}$ s$^{-1}$; an "average" of $(2.6\pm0.4\pm0.5)\times10^{-5}$ ph cm$^{-2}$ s$^{-1}$ has been derived (Vink 2005). An upper limit from INTEGRAL/SPI reported from first studies is consistent with this flux value, and may suggest that the $^{44}$Ti line is broader than 1000 km s$^{-1}$ (Vink 2005).

COMPTEL's sky survey allowed for mapping of the plane of the Galaxy in the $^{44}$Ti line (Dupraz et al. 1996;

Iyudin et al. 1999). Secondary features in these COMPTEL $^{44}$Ti maps kept the discussion about statistical significances and systematic uncertainties alive (see Schönfelder et al. 2000, for a comparison of Cas A to RX J0852, a promising second source candidate, Iyudin et al. 1998). The COMPTEL point source detection algorithm (de Boer et al. 1992) has been tested with simulations over the full sky: likelihood statistics has been verified to reproduce the expected number of artificial sources for a full sky survey, as the noise level is approached. The problem is that in the range of all the $^{44}$Ti gamma-ray lines, all gamma-ray telescopes suffer from a large background from local radioactivity induced by cosmic-ray bombardment of the instruments (Gehrels & Michelson 1999; Weidenspointner et al. 2002). Determination of this background is crucial. For an imaging instrument, this can be done rather well by interpolation of imaging signatures from adjacent energies. But furthermore, for COMPTEL the 1.157 MeV line of $^{44}$Ti is not far above its lower energy threshold, and in fact imaging selections strongly affect the sensitivity of the instrument up to $\simeq$1.5 MeV. Nevertheless, imaging analysis in adjacent energy bands should all experience similar problems, and therefore differences between images in the $^{44}$Ti band and in neighboring energy bands can be attributed to $^{44}$Ti rather than continuum sources or instrumental artifacts, once they are confirmed to be point-like sources (instrumental background lines would in general spread over data space and hence lead to extended or large-scale artifacts in the image, hence impact on the flux measurement rather than on point source detection). Detailed comparisons of results for different energy bands, data subsets, and selections have led to the more cautious report about the Vela-region source (Schönfelder et al. 2000), so that still no convincing second $^{44}$Ti source clearly above the noise level is claimed. The INTEGRAL limits for $^{44}$Ti lines from the Vela region source are now close to the reported COMPTEL flux value for this candidate source (Renaud 2004; von Kienlin et al. 2004) and we therefore consider only one single $^{44}$Ti source (Cas A) as being detected down to flux levels of $10^{-5}$ ph cm$^{-2}$ s$^{-1}$.

For the low-energy lines measured by other instruments, in addition to the instrumental background the underlying continuum (see The et al. 1999 for Cas A) presents a major source of uncertainty (see Vink et al. 2001; Vink & Laming 2003; Vink 2005). This becomes even more of a problem for recombination line features from $^{44}$Sc at 4.1 keV, which have been studied with ASCA (Tsunemi et al. 2000; Iyudin et al. 2005), yet without clear detections (though tantalizing hints have been discussed for the Vela-region source).

For our quantitative comparisons of the $^{44}$Ti supernova rate with the historical record of supernovae in the last millennium (see Appendix B.2), we make use of the COMPTEL survey. We avoid the regions where reduced exposure might eventually lead to increased artifact levels, and concentrate on the inner Galaxy where exposure for the COMPTEL sky survey is deep and homogeneous. We also avoid using data after the second re-boost of the satellite, whereafter the activation level of $^{22}$Na had increased substantially (Weidenspointner et al. 2002). This leaves us with a dataset covering the sky range of $|l| \leq 90°$, $|b| \leq 30°$ using 7 years of the 9-year sky survey. In these gamma-ray data, the $^{44}$Ti source sensitivity should be rather well-behaved and useful for our study. Note that the first inner-Galaxy survey from INTEGRAL (longitudes of $\pm 20°$ around the GC) (Renaud 2004) is consistent with our dataset in that also there no source is found to flux levels of $10^{-5}$ ph cm$^{-2}$ s$^{-1}$ (Renaud 2005).

### 3.2. Galactic supernova rate

Many determinations of the galactic star formation rate (*SFR*) and supernova rate (*SNR*) have been made in past decades (see Diehl et al. 2005 for a compilation of estimates, and Stahler & Palla 2005 on general astrophysical aspects of star formation). In this work we are concerned with the $^{44}$Ti from supernovae, so we need the formation rate of massive stars (above, say, 10 $M_\odot$). The conversion between *SNR* and *SFR* is a sensitive function of the Initial Mass Function (IMF), and values given in the literature thus vary depending on the author's chosen IMF. For a generic transformation equation, we use the calibration from McKee & Williams (1997): $SFR = 196\ SNR$, where the *SFR* is measured in $M_\odot\,\mathrm{yr}^{-1}$ and the *SNR* in events per year. A star formation rate of 4 $M_\odot\,\mathrm{yr}^{-1}$ thus corresponds to a supernova rate of two events per century. These rates only include core collapse supernovae (type II and Ibc), but not SNIa. Generally these supernova rates are averages over time scales much longer than $^{44}$Ti decay.

Many papers discuss the star formation (rate) history (SFH) in relative terms, or the star formation rate surface density ($M_\odot\,\mathrm{yr}^{-1}\,\mathrm{kpc}^{-2}$) in the solar neighborhood and its radial dependence. None of these papers is useful (for our purpose) without an absolute calibration, based on a model of the galactic distribution of star formation.

Generically, the *SFR* is obtained from a tracer that can be corrected for observational selection effects and is understood well enough so that possible evolutionary effects can be taken into account. One either deals with a class of residual objects, such as pulsars or supernova remnants, or with reprocessed light, such as free-free, H-alpha, or IR emission that follows from the ionization and heating of interstellar gas and its dust content in the vicinity of the hot and luminous stars. One must be careful to include time-dependent effects, as the afterglow of an instantaneous starburst behaves differently than the steady state output from a region with continuous star formation. Here, we are concerned with an average star formation rate.

To set the stage, let us collect *SFR* values from the literature. Smith et al. (1978) concluded $SFR = 5.3\ M_\odot\,\mathrm{yr}^{-1}$, while Talbot (1980) finds a very low value $SFR = 0.8\ M_\odot\,\mathrm{yr}^{-1}$, and Guesten & Mezger (1982) report a very high value of $SFR = 13.0\ M_\odot\,\mathrm{yr}^{-1}$. Later papers appear to converge on a median value: Turner (1984) finds $SFR = 3.0\ M_\odot\ \mathrm{yr}^{-1}$, and Mezger (1987) finds $5.1\ M_\odot\,\mathrm{yr}^{-1}$. Measurements in the past decade confirm this moderate rate: McKee (1989) derives $SFR = 3.6\ M_\odot\,\mathrm{yr}^{-1}$ from the analysis of thermal radio emission (free-free) from HII regions around massive stars. This emission is directly proportional to the production rate of ionizing photons, which in turn is directly proportional to the *SFR*. He pointed out that this method is very sensitive to the slope of the high-mass IMF. We also note that the method depends on

stellar model atmospheres in conjunction with models for massive stars, which change with treatments of mass loss, rotation, and convection. This paper also briefly discusses the use of the far-IR luminosity, due to warm dust heated by the absorption of photons from massive stars. The author uses the measured IR luminosity of the Galaxy of $4.7 \times 10^9\ L_\odot$ (from Mezger 1987) to derive $SFR = 2.4\ M_\odot\ \mathrm{yr}^{-1}$.

We must convert between star formation rate (*SFR*) and supernova rate (*SNR*) (see above). McKee & Williams (1997) promote the value $SFR = 4.0\ M_\odot\ \mathrm{yr}^{-1}$, and based on the Scalo's IMF (Scalo 1986) convert this rate into a total number rate of 7.9 stars per year. They assume that all stars above 8 $M_\odot$ become supernovae, corresponding to a supernova fraction of $2.6 \times 10^{-3}$. The mean stellar mass is $\langle m \rangle = 0.51\ M_\odot$. The corresponding cc-SN rate is 2 per century. This value is also supported by a completely independent method, based on the production of radioactive $^{26}$Al in cc-SNe, which can be traced though its gamma-ray line at 1.809 MeV. Timmes et al. (1997) use this method and conclude $SFR = (5 \pm 4)\ M_\odot\ \mathrm{yr}^{-1}$, utilizing the $^{26}$Al line flux derived from COMPTEL. The steady-state mass of $^{26}$Al obtained in their work is in the range 0.7–2.8 $M_\odot$, consistent with the value presented in the recent study by Diehl et al. (2005). Based on the Salpeter IMF in the range 0.1–40 $M_\odot$ and the $^{26}$Al yields from Woosley & Weaver (1995) [which do not include contributions from the Wolf-Rayet wind phase] the authors derive the above quoted *SFR* and an associated cc-supernova rate of 3.4 $\pm$ 2.8 per century. They neglect hydrostatically produced $^{26}$Al that is injected into the ISM in massive star winds, which causes their *SFR* to be overestimated. The large uncertainty is mostly due to the steady-state mass of $^{26}$Al inferred from the COMPTEL flux. INTEGRAL data presented by Diehl et al. (2005) have significantly reduced the error in this key quantity, and with wind yields included the latter study finds $SNR = 1.9 \pm 1.1$ supernovae per century, which corresponds to $SFR = 3.8 \pm 2.2\ M_\odot\ \mathrm{yr}^{-1}$, similar to the value given in McKee & Williams (1997). This *SFR* is very similar to the one obtained for M 51 (Calzetti et al. 2005), and thus places the Galaxy in the group of quiescently star-forming galaxies.

The most recent paper addressing this issue is by Reed (2005), who does not derive the *SFR*, but states that the galactic supernova rate is estimated as probably not less than 1 nor more than 2 per century. Using the conversion factors from McKee & Williams (1997), one infers that the *SFR* is in the range 2–4 $M_\odot\ \mathrm{yr}^{-1}$. Reed uses a sample of a little over 400 O3-B2 dwarfs within 1.5 kpc of the Sun to determine the birthrate of stars more massive than 10 $M_\odot$. The galaxy wide rate is derived from this local measurement by extrapolation based on models for the spatial distribution of stars, a model for galactic extinction (to accomplish corrections for stellar magnitudes), and a model of stellar life times. Reed emphasizes various sources of errors, such as lacking spectral classifications of some bright OB stars, the (poorly known) inhomogeneous spatial structure of extinction as well as stellar density, and non-unique connection between mass and spectral type. Finally, Reed also draws attention to the fact that one would have to include B3 dwarfs as well, if the lower mass limit for supernovae is 8 $M_\odot$ and not 10 $M_\odot$ (see Heger et al. (2003) for comments on this mass limit). The OB-star catalog of the author was used to perform a modified $V/V_{\max}$ test to obtain a present-day star count as a function of absolute $V$-band magnitude. From the stellar life times, and the assumption of steady state, the local birthrate follows. A double exponential model (in galactocentric radius and scale height above the plane) of the spatial distribution of these stars (which includes an inner hole of radius $R = 4.25$ kpc) ultimately leads to a total birthrate of 1.14 OB stars per century. Variations in the size of the hole change this number significantly, which leads the author to finally claim a rate of 1–2 supernovae per century.

In the context of our interpretation of the $^{44}$Ti observations, we would argue that Supernova rates between one and three cc-SNe per century are consistent with the large set of studies reviewed above. To solve the $^{44}$Ti Sky conflict with a choice of the *SNR* (or *SFR*), an extremely low rate outside this range would of course explain the absence of $^{44}$Ti gamma-ray line sources in the sky. However, chemical evolution arguments for $^{44}$Ca would then require correspondingly higher $^{44}$Ti yields which are not supported by explosive nucleosynthesis studies (as discussed below) and which in any case would lead to higher fluxes from supernova remnants and thus again to a source count that exceeds the observed count of ∼1. The observational constraints are on the product of rate and yield. The natural solution to the problem may be the very rare events with extremely high yields, which is discussed below. In that case it is of course totally unclear what to use for the spatial distribution of these events, and "unusual" positions of a gamma-ray line source on the sky (such as that of Cas A) would be hard to interpret.

But perhaps we have overlooked another option. We know that the galactic star formation process is strongly correlated in space and time (Elmegreen et al. 2003). Could it be that the Galaxy just had a brief hiatus in its *SFR*? It would not take too much of a pause (say a few centuries) to explain the absence of bright $^{44}$Ti sources if the past few centuries were very untypical with respect to the *SFR* (or *SNR*). This possibility is included in our Monte Carlo simulations, which show that this is not a likely solution when one simply considers Poisson fluctuations. This solution is thus not acceptable, unless one can point out a physical cause of the hiatus in the recent *SFR*.

### 3.3. Galactic supernovae locations

Likewise, we may wonder about the possibility of very large spatial fluctuations. Could it be that the recent Galaxy exhibits an average star formation, rate-wise, but a lopsided distribution in space. If the opposite side of the Galaxy currently forms stars, and regions in the solar sector are relatively inactive ($l = 90$–$270°$), we expect to detect fewer gamma-ray line sources (because of their somewhat larger average distances). But at the same time the supernovae would also suffer from enhanced extinction, and matching the historic SN record would require a much higher rate. We have simulated the effects of a lopsided profile with a von Mises Distribution, the analog of a Gaussian distribution for circular data (Mardia 1975; Fisher 1996). This function allows us to change from an

axis-symmetric galactic distribution to a one-parameter distribution (measured by a parameter $k$, where $k = 0$ corresponds to the uniform circular distribution) in a chosen direction which we choose it to be the longitude $l = 0°$ direction. We re-simulated the $10^5$ Galaxies sample as described in Sect. 2.5, and find that the detection probabilities (stated in the caption of Fig. 2) change to 0.0042, 0.023, and 0.062 for parameter $k = 0.5$ and 0.0068, 0.035, and 0.087 for parameter $k = 1.0$, respectively. The probability curves for $^{44}$Ti $\gamma$-line source detection (see Fig. B.4) are shifted towards higher rates, as expected, but the overall likelihood of these models decreases. The constraint from the historic record demands new rates that are even larger, as the extinction correction affects the results more strongly than the $D^{-2}$ distance effect for the flux. The combination of these two constraints make lopsided models less acceptable than axis-symmetric ones.

A lopsided model would also make Cas A even more special, regarding its unexpected location on the sky. To alleviate this problem we simulated lopsided star-forming galaxies in which the solar sector was the more active. The detection probabilities of 0, 1, and 2 $^{44}$Ti sources of this model are 0.0005, 0.003, and 0.012 for parameter $k = 1.0$, respectively. This shows that the number of the most probable $^{44}$Ti $\gamma$-line source detection in the Galaxy is >2 detections and the model is less probable than the model used for Fig. 2 for consistency with the observed $^{44}$Ti sky.

Is it reasonable at all to consider one-sided star forming galaxies? That major merger events should be able to tidally induce a lopsided starburst activity is perhaps obvious, but the Galaxy is not undergoing such an event. However, Rudnick et al. (2000) have shown that even minor mergers (Ibata et al. 1995) generically termed "weak interactions" may lead to a boost in the star formation rate correlated with their lopsidedness. Another mechanism for the creation of non-symmetric star formation patterns is the interaction between odd numbers of spiral density waves, as it may be at work in M 51 (Henry et al. 2003). We do not advocate such an asymmetry for our Galaxy, but just wanted to consider this real possibility as one of the potential fixes for the $^{44}$Ti sky problem. Our simulations indicate that even such an extreme solution does not work, as the various combined constraints operate against each other. While a lopsided Galaxy helps on the gamma-ray source count side, the historic record is harder to explain if recent supernovae are located preferentially on the far-side.

### 3.4. Galactic extinction map

Analyzing the consistency of the supernova rates derived from the Galactic historical record and the COMPTEL's gamma-ray map (Appendix B.4), the consistency would improve if the SN rate from historical record is smaller. This could be realized if the true Galactic extinction map is lower than the visual extinction map we used here. Recently there are two published Galactic extinction maps that are useful for the type of study of this paper. The optical reddening model of Mendez & van Altena (1998), which is based on Galactic dust distribution model, makes use of the same optical sky surveys implemented by Hakkila et al. (1997) in addition to some other restricted surveys. However this extinction map is reliable only for solar neighborhood within 6 kpc. Another large scale three-dimensional model of Galactic extinction based on the Galactic dust distribution of Drimmel et al. (2003) has been shown to give a good agreement with the empirical extinction derived from NIR color–magnitude diagrams within 0.05 mag and furthermore it is reliable for a distance up to $\simeq$8 kpc. This extinction model gives a larger magnitude of extinction than that of Hakkila et al. (1997) for longitude $|l| \leq 1.5°$and for most pointing directions from the Sun for distance larger than 6 kpc. For distance less than 5 kpc, the extinction of this map is smaller than that of Hakkila et al. (1997) which could give a better agreement between the SN rates of the historical record and of the COMPTEL's gamma-ray map.

### 3.5. The SN model

#### 3.5.1. Lifetime of $^{44}$Ti

Although the lifetime of $^{44}$Ti measured in laboratories had exhibited a large uncertainty since its first measurement in 1965, a compilation of five recent experiments performed after 1998 gives an averaged lifetime of 87 ± 1 yr, where the quoted error is of statistical and of one standard deviation (see, e.g., Fig. 5 of Hashimoto et al. 2001 and also Görres et al. 1998). Apparently, this small uncertainty in the measured $^{44}$Ti lifetime does not affect the discrepancy discussed here.

It is noted that the above-mentioned lifetime measured in laboratories is for neutral atoms. Since $^{44}$Ti is a pure orbital-electron-capture decay isotope, its lifetime depends on the electronic environment in the evolutional course of a supernova remnant. For example, a fully-ionized $^{44}$Ti is stable, and the lifetime of $^{44}$Ti in the Hydrogen-like ionization state becomes longer by a factor of 2.25 than that of the neutral $^{44}$Ti (see Motizuki & Kumagai 2004). Let us briefly consider the effect of $^{44}$Ti ionization on our problem.

In young supernova remnants, the reverse shock propagates inward through the ejecta and the resulting increase in temperature and density may lead to highly ionized ejecta material through thermal collisions with free electrons. A high-degree of ionization may then result in a longer lifetime of $^{44}$Ti, which would significantly alter the inferred $^{44}$Ti mass. In fact, H-like and He-like Fe ions have been observed in Cas A (see, e.g., Hwang et al. 2004). Because the electron binding energies of Ti are smaller than those of Fe, it is easier to ionize Ti than Fe. Accordingly, $^{44}$Ti atoms in Cas A may be expected to be in such high ionization states at least in part if they are accompanied by the highly ionized Fe (this is expected because $^{44}$Ti is synthesized at the same location as where $^{56}$Ni is also produced in the innermost region of a supernova).

Since the present-day radioactivity was entirely affected by the history of various ionization stages and their duration time for which the $^{44}$Ti has experienced through the evolution, detailed discussion requires numerical simulations as was done by Mochizuki et al. (1999) and Mochizuki (2001). However, we can get a rough idea of the ionization effect on the

radioactivity by using the result of simple linear analysis, i.e., Eq. (7) of Motizuki & Kumagai (2004):

$$\Delta F_\gamma / F_\gamma = (t/\tau - 1)\Delta\tau/\tau, \quad (1)$$

where we have replaced the radioactivity $A$ and the decay rate $\lambda$ appeared in Eq. (7) of Motizuki & Kumagai (2004) with the $\gamma$-ray flux $F_\gamma$ and the $^{44}$Ti lifetime $\tau$, respectively. In Eq. (1), $t$ is the age of a *SNR*, $\Delta F_\gamma$ is the change of the flux by ionization, $\Delta\tau$ is that of the lifetime.

Note that $\Delta\tau$ is always positive because the ionization always increases its lifetime. As was pointed out by the above authors, the sign of $\Delta F_\gamma$ is then determined by that of the term in the parenthesis in the right-hand side of Eq. (1). This means that the flux is *enhanced* by the ionization when a *SNR* is *older* than the $^{44}$Ti lifetime, and that the flux is *reduced* when it is *younger*.

Our concern here is whether the effect of ionization on the lifetime of $^{44}$Ti in *SNR*s can reduce the disagreement between the observed $^{44}$Ti Galactic map and the model's map or not. From the above arguments, we can easily understand that the discrepancy may be diminished if the $\gamma$-line fluxes in Fig. 2 could be smaller which may be realized if most of the $\gamma$-ray detected *SNR*s in Fig. 2 are younger than the $^{44}$Ti lifetime.

To get a rough idea, we performed a calculation in which all parameters are the same as employed for Fig. 2 except 1) the fluxes are multiplied by a factor 0.5 for *SNR*s with ages less than 100 y, and 2) the fluxes are multiplied by a factor 2 for *SNR*s with ages between 200 and 400 y. The selection of 200–400 years old *SNR*s as enhanced targets here is because the effect of the ionization due to the reverse shock is considered to be distinguished for these ages and the further inclusion of the enhanced-flux effect on *SNR*s older than 400 y only makes the discrepancy larger (see Mochizuki et al. 1999 for details). Simulating a $10^5$ galaxy sky, we found that a $\gamma$-ray detector with a detection limit of $1 \times 10^{-5}$ ph cm$^{-2}$ s$^{-1}$ would have a probability of detecting 0, 1, 2 $^{44}$Ti sources of 0.0012, 0.008, and 0.026, respectively. Therefore, from this simple analysis it is suggested that the disagreement cannot be compensated by the ionization effect; in effect it becomes worse in our simple calculations above than the reference calculations of Fig. 2.

A more precise estimate requires the knowledge of the temperature and the density evolution of a supernova remnant, and the distribution of $^{44}$Ti in it. However, any detailed calculations taking into account the retardation of $^{44}$Ti decay due to ionization will not alter the situation better: in any case, the older *SNR*s whose fluxes may be enhanced always dominate in number the younger *SNR*s whose fluxes may be decreased.

### 3.5.2. Nucleosynthesis reaction rates

Estimates of yields of $^{44}$Ti from nucleosynthesis in supernovae depend crucially on key nuclear reaction rates, and uncertainties in these rates limit our ability to constrain the supernova rate. The et al. (1998) studied the sensitivity of $^{44}$Ti yields in alpha-rich freezeouts to uncertainties in nuclear reaction rates. They did this by computing the alpha-rich freezeout with reference values for the reaction rates and then comparing these results with ones from calculations with individual rates varied upwards and downwards by a factor of 100 from their reference values. The results were that the production of $^{44}$Ti was most sensitive to the rates for the following reactions: $^{44}$Ti$(\alpha,\mathrm{p})^{47}$V, $\alpha(2\alpha,\gamma)^{12}$C, $^{44}$Ti$(\alpha,\gamma)^{48}$Cr, and $^{45}$V$(\mathrm{p},\gamma)^{46}$Cr for matter with equal numbers of neutrons and protons ($\eta = 0$). For neutron excess $\eta$ greater than zero, the importance of the reaction $^{45}$V$(\mathrm{p},\gamma)^{46}$Cr drops, but other reactions become more important. In particular, these reactions are $^{12}$C$(\alpha,\gamma)^{16}$O, $^{40}$Ca$(\alpha,\gamma)^{44}$Ti, $^{27}$Al$(\alpha,\mathrm{n})^{30}$P, and $^{30}$Si$(\alpha,\mathrm{n})^{33}$S.

For our purposes, the relevant question is how much the $^{44}$Ti may vary from current supernova models given these uncertainties. Motivated by the work of The et al. (1998), Sonzogni et al. (2000) measured the cross section for the $^{44}$Ti$(\alpha,\mathrm{p})^{47}$V reaction at the astrophysically relevant energies. They found that the experimental cross section for this reaction was a factor of two larger than in the rate compilation of Thielemann et al. (1987) used in the The et al. (1998) calculations. From this result, Sonzogni et al. (2000) inferred a 25% reduction in the amount of $^{44}$Ti produced in alpha-rich freezeouts in supernovae. Other of the key reactions found by The et al. (1998) had similar sensitivities of $^{44}$Ti yield to reaction rates; therefore, if other experimental reaction rates are also a factor of ∼2 different from the theoretical calculations, we can expect similar ∼25% effects on the $^{44}$Ti yield. From these results, we might thus conservatively expect the $^{44}$Ti yield to be uncertain by less than a factor of ∼2 due to reaction rate uncertainties. Such a conclusion is supported by the study of the reaction rate sensitivity of nucleosynthesis yields in core-collapse supernovae by Hoffman et al. (1999). These authors compared the yields from core-collapse supernova models using two different reaction rate libraries. For the 15 $M_\odot$ stellar model studied, the two calculations gave $^{44}$Ti yields that agreed to within 20%, in spite of the fact that many individual nuclear reaction rates differed by a factor of two or more between the two rate compilations.

On the other hand, Nassar et al. (2005) have recently measured the $^{40}$Ca$(\alpha,\gamma)^{44}$Ti reaction cross section in the energy range for nucleosynthesis in supernovae. In that energy range, the authors find that the reaction rate is 5–10 times larger than the previously used theoretical rate calculated from a statistical model (Rauscher et al. 2000). This large difference between the experimental rate and the theoretical rate may be due to the fact that the low level density in the $^{44}$Ti compound nucleus limits the applicability of the statistical model for theoretical predictions for the rate of this reaction. In any event, the larger rate increases the yield of $^{44}$Ti by a factor of ∼2 in the stellar models Nassar et al. (2005) explored. Such a large increase in the $^{40}$Ca$(\alpha,\gamma)^{44}$Ti reaction rate may allow normal core-collapse supernovae to account for the solar system's supply of $^{44}$Ca; however, this result would worsen the discrepancy between the observed Galactic $^{44}$Ti gamma-ray flux and our predictions.

### 3.5.3. The supernova explosion model

In core-collapse supernovae, $^{44}$Ti production occurs by the alpha-rich freezeout near the mass cut. The location of the mass cut in the star will then certainly affect the $^{44}$Ti yield. Also

important is the question of whether the simple-minded notion of a mass cut at a single radial shell in the star even makes sense in more realistic models that account for large-scale fluid motions behind the stalled supernova shock prior to the explosion and for stellar rotation. These more realistic models suggest that the material ejected from near the mass cut will in fact be a mixture of parcels that arose from both inside and outside the mass cut. We can certainly expect variations in the entropies of those parcels, which, in turn will have attendant variations in the $^{44}$Ti yield (e.g., Pruet et al. 2005).

For our purposes, the important issue to consider is how much variation can we expect in the $^{44}$Ti yield from differences in the mass cut and multi-dimensional effects. One-dimensional models suggest that typically half or more of the $^{44}$Ti produced during the explosion might fall back on the remnant (e.g, Nassar et al. 2005). Similar results are possible for the multi-dimensional models. It is therefore quite conceivable that yields of $^{44}$Ti from supernovae of the same mass might vary by factors of $\gtrsim$2 simply due to variations in the location of the mass cut or multi-dimensional effects. Of course, if the supernova forms a black hole with mass greater than $\sim$2 solar masses, it will swallow up its innermost material and, thus, most or all of the $^{44}$Ti (and $^{56}$Ni) it produced. Such supernovae would be dim in both visible and gamma radiation. Perhaps the Galactic $^{44}$Ti map is indicating that supernovae over the last few hundred years have been predominantly of this type.

### *3.6. Supernova homogeneity*

Although often taken for granted, homogeneity among supernovae of a type remains an open issue: for thermonuclear supernovae, *light curves* have been found to be fairly similar (Branch 1998). Their successful empirical relative adjustment through a light-curve-decline parameter apparently makes them "standard candles" over the full range of cosmic evolution (this is the basis for the determination of cosmic expansion history, see e.g. Dahlén et al. 2004). The homogeneity of the *r-process elemental abundance pattern* in low-metallicity stars suggests that the r-process, which is commonly attributed to core collapse supernovae, also presents a fairly well-regulated nucleosynthesis environment (e.g. Thielemann et al. 2002). On the other hand, the $^{56}$Ni masses ejected in supernovae appear to scatter, within $\simeq$30% for SNIa (Benetti et al. 2005), and for core collapse events over a wide range from 0.01 to 1 $M_\odot$ (Woosley & Weaver 1995; Woosley et al. 1995; Thielemann et al. 1996), suggesting more variability in the core collapse nucleosynthesis than in thermonuclear explosions (Nomoto et al. 1997; Thielemann et al. 2004). Still, for supernovae of type Ia alternative model types are also discussed that would produce quite distinctly different nucleosynthesis products than central carbon ignition in Chandrasekhar-mass white dwarfs (Nomoto 1982; Livne & Arnett 1995; Woosley & Weaver 1994).

In summary: supernovae of both types are quite homogeneous in some of their characteristics, but anomalies suggest a deeper study of physical regulations and their observational impact.

#### 3.6.1. 2-3D effects in core collapse supernovae

Nagataki et al. (1997) in their explosive nucleosynthesis calculations of 2-D axisymmetric type II supernova found that materials engulfed by energetic shock waves along polar directions undergo higher temperatures (or higher entropy per baryon, Fryer & Heger 2000) to produce a higher amount of $^{44}$Ti than in spherical explosions. Recently, Maeda & Nomoto (2003) also studied hydrodynamics and explosive nucleosynthesis in bipolar supernova/hypernova explosions. Their bipolar models produce a large amount ($>10^{-4}$ $M_\odot$) of $^{44}$Ti and at the same time eject a relatively small amount ($\sim$0.1–0.2 $M_\odot$) of $^{56}$Ni. These features of 2D supernova models inspire Prantzos (2004) to suggest that the "missing $^{44}$Ti" problem (to be in concordance with SN1987A and Cas A observations and also to account for the $^{44}$Ca solar abundance) could be solved by avoiding the overproduction of $^{56}$Ni. More systematic studies are therefore required under variety of progenitor masses, explosion energies, metallicities, and other physical variables. As this 2D effect could elude the discrepancy between the $^{44}$Ti production in spherical supernova models and the amount observed from Cas A *SNR* in gamma-line fluxes and the amount deduced from $^{44}$Ca in solar abundance, the axisymmetric explosion also seems to be the natural consequences of rotation and magnetic field effects during pre-supernova phase (Müller & Hillebrandt 1981; Yamada & Sato 1994) and the neutrino-driven convection (Burrows et al. 1995) for the core-collapse supernovae. Furthermore, evidence to support the axisymmetric explosion have been inferred from the measurements of pulsar velocities (Burrows & Hayes 1996; Hobbs et al. 2004) and from the jet features observed in radio and X-ray images from several supernova remnants (Gaensler et al. 1998). With various degrees of Rayleigh-Taylor instabilities that may develop in core-collapse supernova (either in 2-D or 3-D simulations), we expect there would be a wide distribution of $^{44}$Ti production in supernova events as inferred indirectly by the pulsar velocity distribution. Thereby the task is to find $^{44}$Ti distribution production with supernovae synthesizing higher than typical amount of $^{44}$Ti produced in a spherical model (to explain the amount of $^{44}$Ca in solar abundance and Cas A *SNR*), but also produces small amount of $^{44}$Ti for the most-recent supernova so their gamma-line emissions are too weak to be detected. For this, we have to wait until the explosive 3-D nucleosynthesis can be performed within reasonable time.

#### 3.6.2. Rare $^{44}$Ti rich events

The apparent deficit of $^{44}$Ti remnants from typical supernovae as the main source of $^{44}$Ca is explained if typical supernovae are not the main source. Some rare type of event with a proportionately higher $^{44}$Ti yield could be the major source and not leave detectable remnants today (e.g., Woosley & Pinto 1988). For example, these could be He-triggered sub-Chandrasekhar-mass thermonuclear supernovae (Woosley & Weaver 1994). If their recurrence time is several times the $^{44}$Ti lifetime, the Poisson probability of having none detectable now can be large. Woosley & Weaver (1994) find some models with up to one hundred times higher $^{44}$Ti yields than the typical supernova

values discussed above. These need only occur now every one to two thousand years to provide the necessary $^{44}$Ca synthesis. Such a scenario, while potentially invisible to gamma-ray astronomy, would imply inhomogeneities among the relative abundances of $^{44}$Ca and other isotopes (see Sect. D.3). A galactic survey at 6.9 keV could test this scenario (Leising 2001). Another $\alpha$-rich freezeout nucleus, $^{59}$Cu, decays to $^{59}$Ni whose half-life is 75 000 years. The nearest remnants of these rare objects from the past $10^5$ years could be easily detectable in the subsequent cobalt $K_\alpha$ X-rays.

Mainstream SiC grains, however, argue against rare producers of large amounts of $^{44}$Ti being responsible for most of Galactic $^{44}$Ca, as the $^{44}$Ca/$^{40}$Ca ratio in mainstream SiC grains does not vary much from grain to grain; here sample size is much larger than for X grains, so a more representative sampling may be assumed (see Appendix D).

We perform a simple simulation to test the viability of the rare-event scenario. In this model, we take the model that produces Fig. B.4 (where the amount of $^{44}$Ti in supernovae are as produced by the supernova models explained in Sect. 2.5) but modify the 10% of core-collapse supernovae to produce 20× the $^{44}$Ti of the supernova models. Therefore on average the amount of $^{44}$Ti in this model is about a factor 2.7 of the model shown in Fig. B.4 to account for the $^{44}$Ca solar abundance. This model gives a better agreement with the observed $^{44}$Ti sky than the model used to produce Fig. 2 where all supernovae produce 3× the amount of $^{44}$Ti of supernovae models. As shown in the caption of Fig. 2, the probability of this model detecting 0, 1, and 2 $^{44}$Ti sources are 0.012, 0.053, and 0.12, respectively. This results show that the model is more probable than the model of Fig. 2 in explaining why COMPTEL and INTEGRAL only detect one $^{44}$Ti source (less than expected). For comparison, the supernovae recurrence rates of the peak of the probability curve of the 1.157 MeV $\gamma$-line fluxes that are consistent with the COMPTEL observed fluxes (see Appendix B.2 and the dotted curve in Fig. B.4) for the model of Fig. B.4, this model, and the model of Fig. 2 are 36 yr (Fig. B.4), 40 yr, and 58 yr, respectively. This result is encouraging that a set of supernovae models with a rare type supernova that produces most of the solar $^{44}$Ca gives a closer recurrence rate to the one implied by the historical supernova record (∼17 yr) than the model with 3× amount of $^{44}$Ti of the calculated supernova models. Still we have no good explanation for why some small number of supernovae are so rich in $^{44}$Ti.

## 4. Conclusions

The observed distribution of pointlike sources of $^{44}$Ti in our Galaxy is inconsistent (at a probability near $10^{-3}$) with the combined current understanding of $^{44}$Ti production, specifically

- core collapse supernovae eject $10^{-4}$ $M_\odot$ of $^{44}$Ti, within a factor of two, and
- the galactic core collapse SN rate is about 3 per century,

assuming the last few centuries are representative of the steady-state $^{44}$Ti production. The inconsistency is exacerbated if we further demand, as currently understood to be so, that the standard solar abundance of $^{44}$Ca originates from $^{44}$Ti-producing supernovae. The larger discrepancy is because the product of the above two quantities falls short by a factor of three of the requisite current $^{44}$Ca production rate. The disagreement persists for any combination of rate and yield whose product is the required value, unless the yield of $^{44}$Ti is very much higher and the rates very much lower, i.e., $^{44}$Ca is not made primarily by typical supernovae events, but by very rare ones. These might include He-triggered detonations of sub-Chandrasekhar SNe Ia, or rare variants of core collapses, perhaps those most departing from spherical symmetry. Evidence of He-cap SNIa as source of the $^{44}$Ca abundance might be identifiable in $^{44}$Ca/$^{40}$Ca ratios greater than solar in some mainstream SiC grains.

A future survey with gamma-ray line sensitivity of $10^{-6}$ cm$^{-2}$ s$^{-1}$ would be expected to detect ≥10 sources (Fig. 2), and so could rule out $^{44}$Ca production by frequent supernovae at confidence $5 \times 10^{-5}$. Regardless of specific assumptions, the Cas A supernova remnant as the brightest $^{44}$Ti remnant in the galaxy is a priori very unlikely. That the brightest *SNR* should be found in the outer galaxy or that it is over 300 years old are each improbable. It suggests that yields higher than suggested by many current calculations are possible, which, of course, makes the lack of other detectable remnants even more puzzling.

*Acknowledgements.* Part of this work was supported by NASA Grant NAG5-6892, NAG5-13565, NAG5-10764 to Clemson University and DOE's Scientific Discovery through Advanced Computing Program (grant DE-FC02-01ER41189). Research by DDC was supported by NASA's Origin of Solar Systems Program.

## References

Ahmad, I., Bonino, G., Castagnoli, G. C., et al. 1998, Phys. Rev. Lett., 80, 2550
Amari, S., & Zinner, E. 1997, in Astrophysical Implications of the Laboratory Study of Presolar Materials, 287
Arnett, D. 1996, in IAU Colloq., 145, Supernovae and Supernova Remnants, 91
Badenes, C., Bravo, E., Borkowski, K. J., & Dominguez, I. 2003, ApJ, 593, 358
Badenes, C., Borkowski, K. J., Hughes, J. P., Hwang, U. & Bravo, E., 2005 [arXiv:astro-ph/0511140]
Bahcall, J. N., & Soneira, R. M. 1980, ApJS, 44, 73
Benetti, S., Cappellaro, E., Mazzali, P. A., et al. 2005, ApJ, 623, 1011
Blair, W. P. 2005, in ASP Conf. Ser. 342: 1604-2004: Supernovae as Cosmological Lighthouses, 416
Branch, D. 1998, ARA&A, 36, 17
Burrows, A. 2000, Nature, 403, 727
Burrows, A., & Hayes, J. 1996, in AIP Conf. Proc. 366, High Velocity Neutron Stars, 25
Burrows, A., Hayes, J., & Fryxell, B. A. 1995, ApJ, 450, 830
Calzetti, D., Kennicutt, R. C., Bianchi, L., et al. 2005, ApJ, 633, 871
Cappellaro, E. 2003, LNP Vol. 598: Supernovae and Gamma-Ray Bursters, 37

Cappellaro, E., Turatto, M., Benetti, S., et al. 1993, A&A, 273, 383
Clayton, D. D. 1975, Nature, 257, 36
Clayton, D. D. 1982, in Essays in Nuclear Astrophysics, 401
Clayton, D. D. 1985, in Nucleosynthesis: Challenges and New Developments, 65
Clayton, D. D. 1988, MNRAS, 234, 1
Clayton, D. D. 2003, ApJ, 598, 313
Clayton, D. D., Amari, S., & Zinner, E. 1997a, Ap&SS, 251, 355
Clayton, D. D., Arnett, D., Kane, J., & Meyer, B. S. 1997b, ApJ, 486, 824
Clayton, D. D., Hartmann, D. H., & Leising, M. D. 1993, ApJ, 415, L25
Clayton, D. D., & Nittler, L. R. 2004, ARA&A, 42, 39
Dahlén, T., Fransson, C., Östlin, G., & Näslund, M. 2004, MNRAS, 350, 253
Dawson, P. C., & Johnson, R. G. 1994, JRASC, 88, 369
de Boer, H., Bennett, K., den Herder, H., et al. 1992, in DATA Analysis in Astronomy – IV P. 241, 241
de Vaucouleurs, G., & Pence, W. D. 1978, AJ, 83, 1163
Deneault, E. A.-N., Clayton, D. D., & Heger, A. 2003, ApJ, 594, 312
Diehl, R., Dupraz, C., Bennett, K., et al. 1995, A&A, 298, 445
Diehl, R., et al. 2005, Nature, to appear
Drimmel, R., Cabrera-Lavers, A., & López-Corredoira, M. 2003, A&A, 409, 205
Dupraz, C., Bloemen, H., Bennett, K., et al. 1997, A&A, 324, 683
Dwek, E. 1998, ApJ, 501, 643
Elmegreen, B. G., Elmegreen, D. M., & Leitner, S. N. 2003, ApJ, 590, 271
Fisher, N. I. 1996, Statistical Analysis of Circular Data (New York, NY: Cambridge University Press)
Fransson, C., & Kozma, C. 2002, New Astron. Rev., 46, 487
Fryer, C. L., & Heger, A. 2000, ApJ, 541, 1033
Görres, J., Meißner, J., Schatz, H., et al. 1998, Phys. Rev. Lett., 80, 2554
Gaensler, B. M., Green, A. J., & Manchester, R. N. 1998, MNRAS, 299, 812
Gehrels, N., & Michelson, P. 1999, Astropart. Phys., 11, 277
Guesten, R., & Mezger, P. G. 1982, Vistas Astron., 26, 159
Hakkila, J., Myers, J. M., Stidham, B. J., & Hartmann, D. H. 1997, AJ, 114, 2043
Hartmann, D., The, L.-S., Clayton, D. D., et al. 1993, A&AS, 97, 219
Hashimoto, T., Nakai, K., Wakasaya, Y., et al. 2001, Nucl. Phys. A, 686, 591
Hatano, K., Fisher, A., & Branch, D. 1997, MNRAS, 290, 360
Heger, A., Fryer, C. L., Woosley, S. E., Langer, N., & Hartmann, D. H. 2003, ApJ, 591, 288
Henry, A. L., Quillen, A. C., & Gutermuth, R. 2003, AJ, 126, 2831
Higdon, J. C., & Fowler, W. A. 1987, ApJ, 317, 710
Hobbs, G., Lyne, A., Kramer, M., & Lorimer, D. 2004, in 35th COSPAR Scientific Assembly, 1152
Hoffman, R. D., Woosley, S. E., Weaver, T. A., Rauscher, T., & Thielemann, F.-K. 1999, ApJ, 521, 735
Hoppe, P., Strebel, R., Eberhardt, P., Amari, S., & Lewis, R. S. 2000, Meteor. Planet. Sci., 35, 1157
Hwang, U., Hughes, J. P., & Petre, R. 1998, ApJ, 497, 833
Hwang, U., Laming, J. M., Badenes, C., et al. 2004, ApJ, 615, L117
Ibata, R. A., Gilmore, G., & Irwin, M. J. 1995, MNRAS, 277, 781
Iyudin, A. 1999, in Astronomy with Radioactivities, 65
Iyudin, A. F., Aschenbach, B., Becker, W., Dennerl, K., & Haberl, F. 2005, A&A, 429, 225
Iyudin, A. F., Diehl, R., Bloemen, H., et al. 1994, A&A, 284, L1
Iyudin, A. F., Schönfelder, V., Bennett, K., et al. 1998, Nature, 396, 142
Iyudin, F. A., Schönfelder, V., Bennett, K., et al. 1999, Astrophys. Lett. Commun., 38, 383
Janka, H.-T., Buras, R., Kifonidis, K., Plewa, T., & Rampp, M. 2003, in From Twilight to Highlight: The Physics of Supernovae, 39
Kennicutt, R. C. 1998, ARA&A, 36, 189
Knödlseder, J. 2000, New Astron. Rev., 44, 315
Leising, M. D. 2001, ApJ, 563, 185
Leising, M. D., & Share, G. H. 1990, ApJ, 357, 638
Leising, M. D., & Share, G. H. 1994, ApJ, 424, 200
Livne, E., & Arnett, D. 1995, ApJ, 452, 62
Lorimer, D. R., & Kramer, M. 2004, Handbook of Pulsar Astronomy, Cambridge observing handbooks for research astronomers, Vol. 4 (Cambridge, UK: Cambridge University Press, 2004)
Lyne, A. G., & Graham-Smith, F. 1998, Pulsar astronomy (Cambridge, UK, New York: Cambridge University Press)
Maeda, K., & Nomoto, K. 2003, ApJ, 598, 1163
Maeder, A., & Conti, P. S. 1994, ARA&A, 32, 227
Mahoney, W. A., Ling, J. C., Wheaton, W. A., & Higdon, J. C. 1992, ApJ, 387, 314
Mardia, K. V. 1975, J. R. Statist. Soc., 37, 349
Matteucci, F. 2003, The Chemical Evolution of the Galaxy (Department of Astronomy, University of Trieste, Italy; Astrophysics and Space Science Library), Vol. 253, reprint (Dordrecht: Kluwer Academic Publishers)
McKee, C. F. 1989, ApJ, 345, 782
McKee, C. F., & Williams, J. P. 1997, ApJ, 476, 144
Mendez, R. A., & van Altena, W. F. 1998, A&A, 330, 910
Mezger, P. G. 1987, in Starbursts and Galaxy Evolution, 3–18
Mihalas, D., & Binney, J. 1981, Galactic astronomy: Structure and kinematics, 2nd edition (San Francisco, CA: W. H. Freeman and Co.), 608
Mochizuki, Y. 2001, Nucl. Phys. A, 688, 58c
Mochizuki, Y., Takahashi, K., Janka, H.-T., Hillebrandt, W., & Diehl, R. 1999, A&A, 346, 831
Motizuki, Y., & Kumagai, S. 2004, New Astron. Rev., 48, 69
Müller, E., & Hillebrandt, W. 1981, A&A, 103, 358
Nagataki, S., Hashimoto, M.-A., Sato, K., & Yamada, S. 1997, ApJ, 486, 1026
Nassar, H., Paul, M., Ahmad, I., et al. 2005, ArXiv Nuclear Experiment e-prints
Nittler, L. R. 2005, ApJ, 618, 281
Nittler, L. R., Alexander, C. M. O., Stadermann, F. J., & Zinner, E. 2005, in 36th Annual Lunar and Planetary Science Conference, 2200
Nittler, L. R., Amari, S., Zinner, E., Woosley, S. E., & Lewis, R. S. 1996, ApJ, 462, L31
Nomoto, K. 1982, ApJ, 257, 780
Nomoto, K., Iwamoto, K., Nakasato, N., et al. 1997, Nucl. Phys. A, 621, 467
Norman, E. B., Browne, E., Chan, Y. D., et al. 1997, Nucl. Phys. A, 621, 92
Pagel, B. E. J. 1997, Nucleosynthesis and chemical evolution of galaxies (Cambridge: Cambridge University Press)
Prantzos, N. 2004, in ESA SP-552: 5th INTEGRAL Workshop on the INTEGRAL Universe, 15
Prantzos, N., & Diehl, R. 1996, Phys. Rep., 267, 1
Pruet, J., Woosley, S. E., Buras, R., Janka, H.-T., & Hoffman, R. D. 2005, ApJ, 623, 325
Rauscher, T., Thielemann, F.-K., Görres, J., & Wiescher, M. 2000, Nucl. Phys. A, 675, 695
Reed, B. C. 2005, AJ, 130, 1652

Renaud, M. 2004, in The INTEGRAL Universe. Proceedings of the 5th INTEGRAL Workshop held at Munich, Germany, 16–20 February 2004, ed. V. Schönfelder, G. Lichti, & C. Winkler, ESA Publications Division, 81
Renaud, M., Lebrun, F., Terrier, R., et al. 2004, in SF2A-2004: Semaine de l'Astrophysique Française, meeting held in Paris, France, June 14–18, 2004, ed. F. Combes, D. Barret, T. Contini, F. Meynadier, & L. Pagani (EDP Sciences, Conf. Ser.), 90
Renaud, R., et al. 2005, New Astron. Rev., to appear
Rothschild, R. E., & Lingenfelter, R. E. 2003, ApJ, 582, 257
Rothschild, R. E., Lingenfelter, R. E., Blanco, P. R., et al. 1998, in The Active X-ray Sky: Results from BeppoSAX and RXTE, 68
Rudnick, G., Rix, H.-W., & Kennicutt, R. C. 2000, ApJ, 538, 569
Scalo, J. M. 1986, in Luminous Stars and Associations in Galaxies, IAU Symp., 116, 451
Schönfelder, V., Bloemen, H., Collmar, W., et al. 2000, in Am. Inst. Phys. Conf. Ser., 54
Scoville, N. Z., Polletta, M., Ewald, S., et al. 2001, AJ, 122, 3017
Smith, L. F., Mezger, P. G., & Biermann, P. 1978, A&A, 66, 65
Sonzogni, A. A., Rehm, K. E., Ahmad, I., et al. 2000, Phys. Rev. Lett., 84, 1651
Stahler, S. W., & Palla, F. 2005, The Formation of Stars (Wiley-VCH), 865
Talbot, R. J. 1980, ApJ, 235, 821
Tammann, G. A., Loeffler, W., & Schroeder, A. 1994, ApJS, 92, 487
Taylor, J. H., & Cordes, J. M. 1993, ApJ, 411, 674
The, L.-S., Clayton, D. D., Jin, L., & Meyer, B. S. 1998, ApJ, 504, 500
The, L.-S., Diehl, R., Hartmann, D. H., et al. 1999, in Astronomy with Radioactivities, 77–84
The, L.-S., Leising, M. D., Kurfess, J. D., et al. 1996, A&AS, 120, C357
Thielemann, F., Argast, D., Brachwitz, F., et al. 2002, in Chemical Enrichment of Intracluster and Intergalactic Medium, ASP Conf. Ser., 253, 205
Thielemann, F., Nomoto, K., & Hashimoto, M. 1996, ApJ, 460, 408
Thielemann, F.-K., Arnould, M., & Truran, J. W. 1987, in Adv. Nucl. Astrophys., ed. E. Vangioni-Flam, J. Audouze, M. Cassé, J.-P. Chieze, & J. Tran Thahn Van (Gif-sur-Yvette: Éditions Frontières), 525
Thielemann, F.-K., Brachwitz, F., Höflich, P., Martinez-Pinedo, G., & Nomoto, K. 2004, New Astron. Rev., 48, 605
Timmes, F. X., & Clayton, D. D. 1996, ApJ, 472, 723
Timmes, F. X., Diehl, R., & Hartmann, D. H. 1997, ApJ, 479, 760
Timmes, F. X., Woosley, S. E., Hartmann, D. H., & Hoffman, R. D. 1996, ApJ, 464, 332
Timmes, F. X., Woosley, S. E., & Weaver, T. A. 1995, ApJS, 98, 617
Tsujimoto, T., Nomoto, K., Yoshii, Y., et al. 1995, MNRAS, 277, 945
Tsunemi, H., Miyata, E., Aschenbach, B., Hiraga, J., & Akutsu, D. 2000, PASJ, 52, 887
Turner, B. E. 1984, Vistas Astron., 27, 303
van den Bergh, S. 1991, in Supernovae. The Tenth Santa Cruz Workshop in Astronomy and Astrophysics, held July 9–21, 1989, Lick Observatory, ed. S. E. Woosley (New York: Springer-Verlag), 711
van den Bergh, S., & McClure, R. D. 1990, ApJ, 359, 277
van den Bergh, S., & McClure, R. D. 1994, ApJ, 425, 205
van den Bergh, S., & Tammann, G. A. 1991, ARA&A, 29, 363
Vink, J. 2004, in 35th COSPAR Scientific Assembly, 4023
Vink, J. 2005, Adv. Space Res., 35, 976
Vink, J., & Laming, J. M. 2003, ApJ, 584, 758
Vink, J., Laming, J. M., Kaastra, J. S., et al. 2001, ApJ, 560, L79
von Kienlin, A., Attie, D., & Cordier, B. 2004, in The INTEGRAL Universe. Proceedings of the 5th INTEGRAL Workshop held at Munich, Germany, 16–20 February 2004, ed. V. Schönfelder, G. Lichti, & C. Winkler, ESA Publications Division, 87
Weidenspointner, G., Harris, M. J., Jean, P., & Diallo, N. 2002, New Astron. Rev., 46, 625
Woosley, S. E., Arnett, W. D., & Clayton, D. D. 1973, ApJS, 26, 231
Woosley, S. E., Hartmann, D., & Pinto, P. A. 1989, ApJ, 346, 395
Woosley, S. E., Langer, N., & Weaver, T. A. 1995, ApJ, 448, 315
Woosley, S. E., & Pinto, P. A. 1988, in Nuclear Spectroscopy of Astrophysical Sources, AIP Conf. Proc., 170, 98
Woosley, S. E., & Weaver, T. A. 1994, ApJ, 423, 371
Woosley, S. E., & Weaver, T. A. 1995, ApJS, 101, 181
Yamada, S., & Sato, K. 1994, ApJ, 434, 268
Yoshii, Y., Tsujimoto, T., & Nomoto, K. 1996, ApJ, 462, 266
Zinner, E. 1998, Ann. Rev. Earth Planet. Sci., 26, 147

# Online Material

## Appendix A: Simulations of $^{44}$Ti skies

### A.1. Monte carlo simulation details

In generating supernova events of our Monte Carlo simulations, we adopt the procedure shown by Higdon & Fowler (1987); Mahoney et al. (1992); Hartmann et al. (1993). A random number between 0 and 1000 is uniformly generated to represent a supernova age between zero and 1000 y ($\simeq 11.4 \times \tau_{\rm Ti44}$) where $\tau_{\rm Ti44} = (87.7 \pm 1.7)$ yr (Norman et al. 1997; Görres et al. 1998; Ahmad et al. 1998) is the mean life of $^{44}$Ti. This range is large enough that a supernova age older than 1000 y does not contribute to the Galactic $^{44}$Ti flux.

Another random number is generated to choose the type of the supernova event. Then, several random numbers are generated to give us the location of the supernova according to its spatial distribution. A detail procedure in generating the locations of supernova from a disk and spheroid populations of type Ia events can be found in the paper of Higdon & Fowler (1987); Mahoney et al. (1992). The distance of the supernova location to the Sun can be calculated easily.

A random number is generated from a Gaussian distribution to give us the peak bolometric magnitude of the supernova following the distribution given in Sect. A.2. The apparent magnitude then can be calculated knowing the location, the distance, extinction magnitude (from Hakkilla et al.'s empirical model), and the peak bolometric magnitude of the supernova. We find in model **A** (Sect. A.2) the fraction of SNe in the last millennium brighter than apparent magnitude 0 is ∼11% (see Fig. B.3).

The amount of $^{44}$Ti of the supernova is given by a uniform distribution of $^{44}$Ti according to its type as described in Sect. 2.5, *however note that the analysis in this appendix does not use the multiplying factor of 3 that is used in 2.5*. $F_\gamma$, the $^{44}$Ti gamma-line flux at the Sun location, then can be determined knowing the location, the distance, the age, and the amount of $^{44}$Ti of the supernova:

$$F_\gamma = 8.21 \times 10^{-3}\ M_4\ \exp(-t/87.7\ {\rm yr})/d_{\rm kpc}^2\ \gamma\ {\rm cm}^{-2}\ {\rm s}^{-1}$$

where $M_4$ is the $^{44}$Ti of the supernova in units of $10^{-4}\ M_\odot$ and $d_{\rm kpc}$ is the distance (in kpc) of the supernova from the Sun. We find that in Model **A** the fraction of supernovae in the simulations with $^{44}$Ti $\gamma$-line fluxes larger than $1 \times 10^{-5}\ \gamma\ {\rm cm}^{-2}\ {\rm s}^{-1}$ and $3 \times 10^{-5}\ \gamma\ {\rm cm}^{-2}\ {\rm s}^{-1}$ are ∼11% and ∼5%, respectively (Fig. 3). Its longitude distribution along the Galactic plane in some relevant $^{44}$Ti gamma-line flux bandwidths can be seen in Fig. 4, while for models **B** and **C** (Sect. A.2) are shown in Fig. A.1.

We generate 1 million supernovae according to the above prescription and construct galaxies with numbers of supernovae between 1 and 300. For each galaxy with a certain $n$ number of supernovae, the $^{44}$Ti gamma-line flux distribution $F(f_\gamma, n)$ and the SN apparent magnitude distributed $M(m, n)$ can be extracted.

For a galaxy with SN recurrence time of $T_{\rm rec}$ or average supernova rate, $\mu = 1000/T_{\rm rec}$ (we only simulate supernova events in the last millennium as described above), the $^{44}$Ti gamma-line flux distribution, $F(f_\gamma, \mu)$ can be obtained from $F(f_\gamma, \mu) = \sum_{n=0}^{\infty} \frac{e^{-\mu}\,\mu^n}{n!}\ F(f_\gamma, n)$.

### A.2. Supernova types and spatial distribution

Supernova events as the source of Galactic $^{44}$Ti can either be type Ia, Ib/c, or II SNe. For this study, we choose a generally accepted (though uncertain) value of the type ratio, Ia:Ib/c:II = 0.1:0.15:0.75 (Dawson & Johnson 1994; Hatano et al. 1997). Yoshii et al. (1996) and Tsujimoto et al. (1995) using their chemical evolution model find that the ratio of the total number of type Ia to type II SNe of 0.12 gives a good agreement with the observed solar abundance. This is consistent with the observed Ia frequency which is as low as 10% of the total SNe occurrence (van den Bergh & Tammann 1991). Monte Carlo representations of type Ia SNe are generated using a nova distribution template that traces the blue light distribution in M 31 (Higdon & Fowler 1987). These populations form an axisymmetric disc and a spherically symmetric bulge. The spheroid density distribution follows:

- $1.25\ (\frac{R}{R_\odot})^{-6/8}\ {\rm e}^{-10.093[(\frac{R}{R_\odot})^{1/4}-1]}$ for $R \le 0.03\ R_\odot$;
- $(\frac{R}{R_\odot})^{-7/8}\ {\rm e}^{-10.093[(\frac{R}{R_\odot})^{1/4}-1]}\ [1 - \frac{0.08669}{(\frac{R}{R_\odot})^{1/4}}]$ for $R \ge 0.03\ R_\odot$;

and the disc density distribution follows:

- $n(\rho, z) \propto {\rm e}^{-|z|/\sigma_z}\ {\rm e}^{-(\rho - R_\odot)/\rho_{\rm h}}$;
- $\sigma_z = 0.325$ kpc (Mihalas & Binney 1981);
- $\rho_{\rm h} = 3.5$ kpc (de Vaucouleurs & Pence 1978);

The fraction of SNIa occurring in the spheroid is taken to be ∼1/7 of the total SNIa (Bahcall & Soneira 1980).

Supernovae of types Ib & II are associated with massive stars whose birth places are exponentially distributed in height above the plane with a scale length of ∼100 pc. Because the rate of core collapses is larger than the rate of thermonuclear supernovae, we study several type II distributions to ensure that our results do not depend significantly on this choice. We consider three cases:

1. model **A**: exponential disk with no supernova within 3 kpc of the Galactic center, with radial scale length of 5 kpc Hatano et al. (1997):
   $n(\rho, z) \propto {\rm e}^{-|z|/\sigma_z}\ {\rm e}^{-\rho/\rho_{\rm d}}$
   $\sigma_z = 0.100$ kpc
   $\rho_{\rm d} = 5.0$ kpc;
2. model **B**: exponential disk with radial scale length of 3.5 kpc that produces an acceptable fit to the COMPTEL's $^{26}$Al $\gamma$-line map Diehl et al. (1995);
3. model **C**: Gaussian-ring disk at radial distance of 3.7 kpc and radial distance scale length of 1.27 kpc (Taylor & Cordes 1993).

The distribution of supernovae in model **A** in directional is shown in Fig. A.2 and in distance from the Sun is shown in Fig. A.3.

## Appendix B: Comparison of supernova rates from $^{44}$Ti gamma-rays and the historical record

In order to produce a consistent picture of the recent Galactic supernova rate with the best known $^{44}$Ti supernova yields, supernovae types and spatial distribution, and Galactic extinction model we utilize our Monte Carlo simulation method to

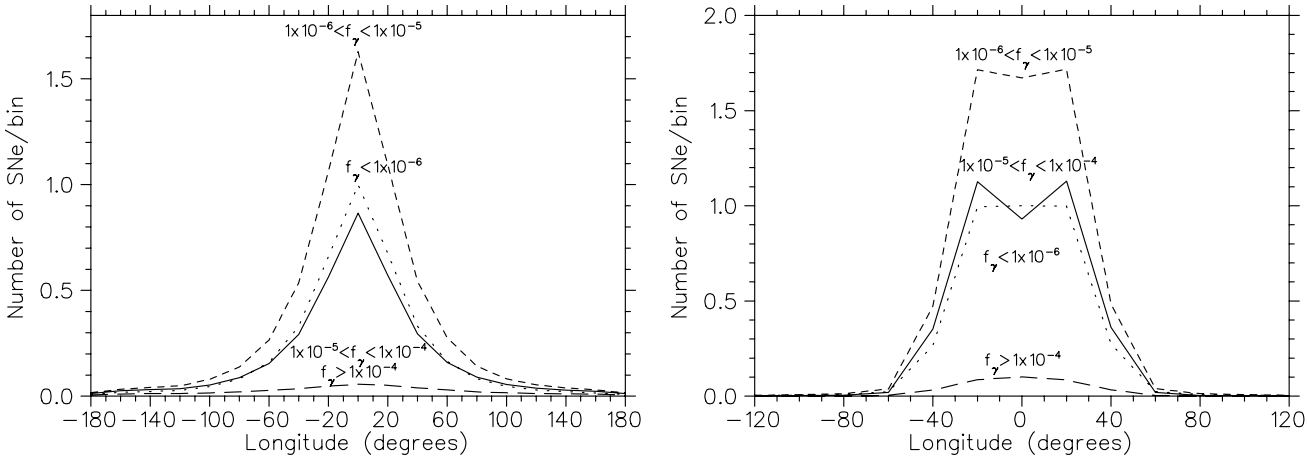


**Fig. A.1.** Same as Fig. 4 but for models **B** (left) and **C** (right).

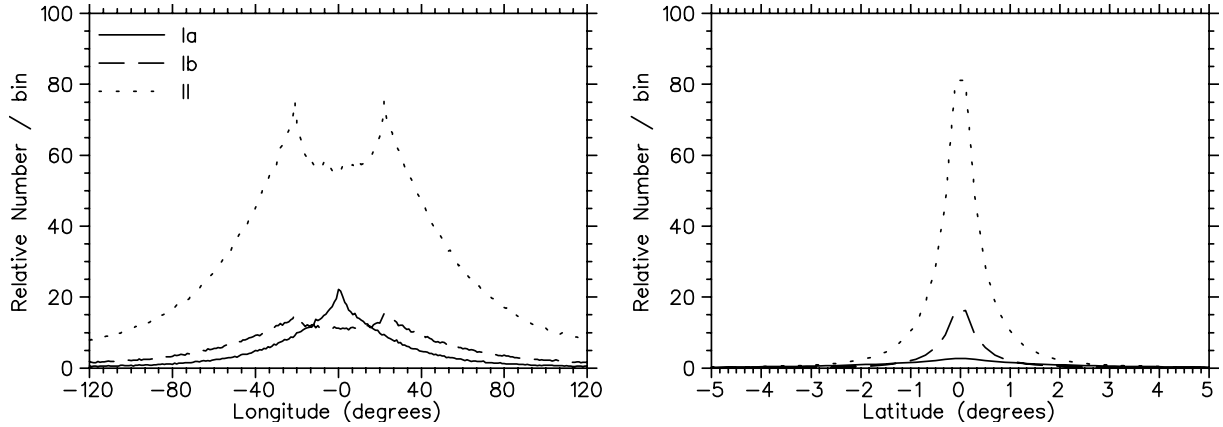


**Fig. A.2.** The distribution of supernovae in model **A** in Galactic longitude and latitude.

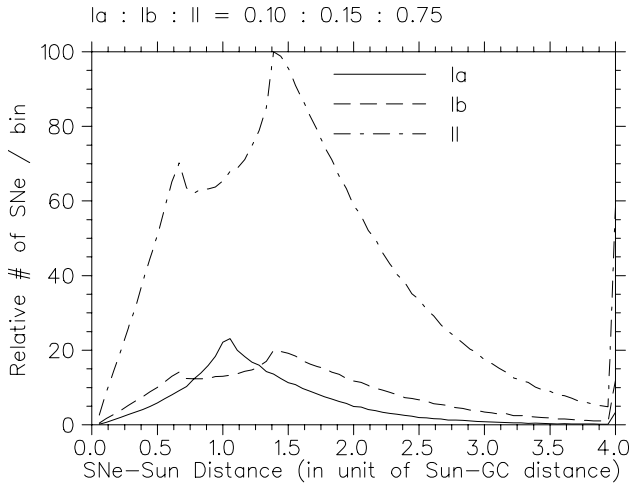


**Fig. A.3.** The distribution of supernovae distance in model **A**.

compare two observables of the same phenomenon (Higdon & Fowler 1987; Mahoney et al. 1992; Hartmann et al. 1993; The et al. 1999). We use the COMPTEL gamma-ray maps and the six historical Galactic supernova record of the last millennium to constrain the range of Galactic supernova rates.

Similar to the above determination of $^{44}$Ti flux distribution from a simulated set of supernova events, other distribution such as the apparent magnitude distribution of supernovae for a galaxy with an average supernova rate $\mu$ can be constructed (Sect. B.3). From this distribution we can determine the probability of optical detection for a certain detection-limiting apparent magnitude, such as magnitude 0, for example. In this way, we can use the same underlying assumptions about supernova characteristics, and compare two different observables, i.e. $^{44}$Ti gamma-ray versus optical detections of the supernovae at the adopted rates. Varying the rates then so that they conform to the observational constraints, we obtain a handle on systematic differences in observed supernova rates through these two observational windows.

For the $^{44}$Ti gamma-ray observations, we utilize the COMPTEL survey discussed above (Sects. 2.1 and 3.1). For the optical observations, we utilize the historical record summarized in Table B.1.

For comparison of the COMPTEL gamma-ray map with the results of Monte Carlo simulations, due to our limited computational power, for the purpose to reduce systematic effects from regions of low exposure, and due to our limited ability to analyze the map, we perform two analysis. In the flux dataspace (Sect. B.2) we use the flux information exclusively, without using the observed location of the gamma-ray source. In the map dataspace analysis (Sect. B.1), we only use the COMPTEL map of inner galaxy ($|l| \leq 90°$, $|b| \leq 30°$) which does not

**Table B.1.** Recent galactic supernova record.

| Name | Year | Distance (kpc) | $l$ | $b$ | Type |
|---|---|---|---|---|---|
| Lupus (SN 1006) | 1006 | 2.2 | 327.57 | 14.57 | Ia |
| Crab | 1054 | 2.0 | 184.55 | −5.79 | II |
| 3C 58 (SN 1181) | 1181 | 2.6 | 130.73 | 3.07 | II |
| Tycho | 1572 | 2.4 | 120.09 | 1.42 | Ia[a] |
| Kepler | 1604 | 4.2 | 4.53 | 6.82 | Ib/II[b] |
| Cas A | 1680 | 2.92 | 111.73 | −2.13 | Ib |

[a] Studies of X-ray emission from Tycho's shocked ejecta show the SNR was created by a type Ia SN (Hwang et al. 1998; Badenes et al. 2003, 2005).
[b] The uncertainty of Kepler's SN Type was reviewed by Blair (2005).

include the locations of the detected $^{44}$Ti $\gamma$-line from Cas A and GRO J0852-4642. In order to see how consistent the model with the Galactic supernova record, we perform the historical record analysis below.

### B.1. Map dataspace analysis

In map (imaging) analysis, a simulated COMPTEL data set is produced by convolving the directions and the $^{44}$Ti $\gamma$-line fluxes of the Monte-Carlo-generated supernovae through the COMPTEL detector response. The probability of the consistency of the simulated data with the measured counts is carried out by calculating the likelihood of the simulated data plus the best-fit background model, and comparing this to the likelihood of the background model only (de Boer et al. 1992). The change in the likelihood gives the relative probability that the specific realization of the model is consistent with the measured COMPTEL data. This process is repeated for at least $10^4$ galaxies to obtain the average relative probability of the model at a particular supernova rate as dashed lines in Figs. B.4, and B.5.

### B.2. Flux dataspace analysis

In flux dataspace analysis, in order to include the detected sources, the locations of the $^{44}$Ti supernovae are not used, flux information is used exclusively. The flux dataspace consists of the two $^{44}$Ti detected fluxes from Cas A *SNR* and GRO J0852-4642 Iyudin et al. (1998) with other fluxes assumed to be zero (with which they are consistent.) For each Monte Carlo Galaxy, a $\chi^2$ value is calculated by comparing the two strongest fluxes with the fluxes measured from Cas A and GRO J0852-4642 and the other fluxes are compared with null fluxes. The probability of the model to be consistent with the COMPTEL fluxes is determined from the $\chi^2$ and using the number of degrees of freedom as the number of independent $10^\circ \times 10^\circ$ image elements (fields of view) of the supernova positions in the model. This size of independent fields of view is obtained by calibrating the size to produce the results of the analysis of COMPTEL's map of the inner Galaxy. Averaging the probabilities of $10^6$ Monte Carlo galaxies, we obtain the average probability shown in Figs. B.4 and B.5 as dotted lines.

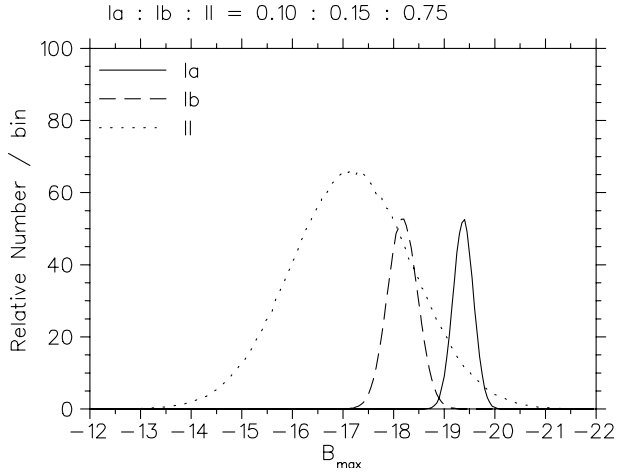


**Fig. B.1.** The distribution of the peak absolute magnitudes of supernova in the $B$-band of model **A**.

### B.3. Historical record analysis

The historical supernova record covering the last millennium shows a total of only six Galactic SNe during that era (Table B.1). Of course, this small number is due to significant losses from extinction and incomplete monitoring of the sky, especially during the early centuries. In fitting this data, we count the fraction of galaxies that have six SNe brighter than magnitude 0. In this approach, we assume that historical SNe were detected if they were brighter than magnitude 0.

The peak absolute magnitudes of supernovae in the $B$-band are approximated by Gaussian distributions. For the mean values and the one standard deviation we adopt for type Ia $M_B = -19.4$, $\sigma = 0.2$ (Branch 1998), for type Ib $M_B = -18.2$, $\sigma = 0.3$ (Dawson & Johnson 1994), and for type II $M_B = -17.2$, $\sigma = 1.2$ (van den Bergh & Tammann 1991). Their distribution is shown in Fig. B.1 Observed magnitudes of simulated SNe are obtained by convolving absolute magnitudes through a Galactic extinction model of (Hakkila et al. 1997). In this extinction model, the total visual extinction from the Sun's location to the Galactic Center is 11.64 mag and the total visual extinction perpendicular to the Galactic plane at Sun's location is ∼0.1 mag (Fig. B.2). The cumulative distribution of supernovae having blue peak apparent magnitude brighter than $m_B$ in model **A** is shown in Fig. B.3.

The average fraction of the model that is consistent with six events brighter than magnitude 0 is shown in Figs. B.4, and B.5 as solid lines.

### B.4. The supernova rates: optical versus gamma-ray constraints

Our Galactic supernova record analysis leads to a most probable Galactic supernova recurrence time of ∼17, ∼16, and ∼13 y based on models A, B, and C, respectively. This implies a larger rate than given by previous investigations based on the historical record. For example, Dawson & Johnson (1994) estimated ∼3 SNe per century as also obtained by Tammann et al. (1994). The rate is smaller than ours because Dawson & Johnson (1994) considered 7 observed SNe within the last

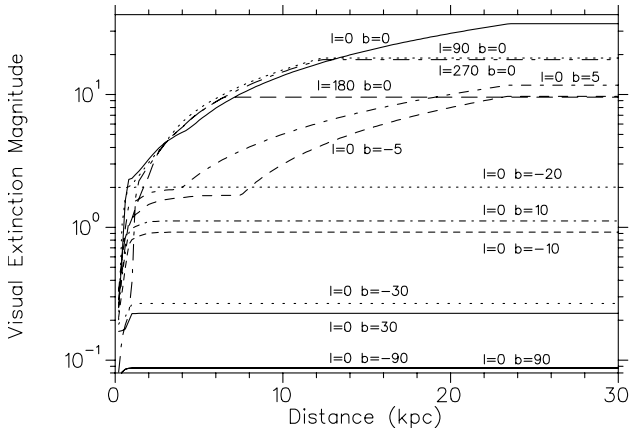


**Fig. B.2.** The Galactic visual extinction magnitude as a function of distance from the Sun to various direction according to empirical model of (Hakkila et al. 1997).

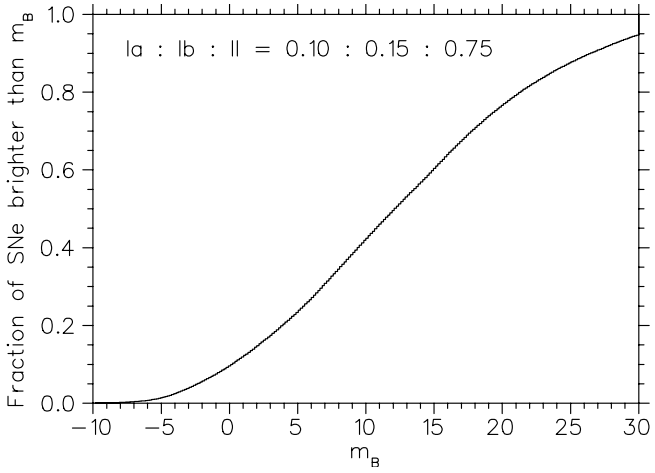


**Fig. B.3.** The apparent magnitude of supernovae in model **A** according to empirical extinction model of Hakkila et al. (1997).

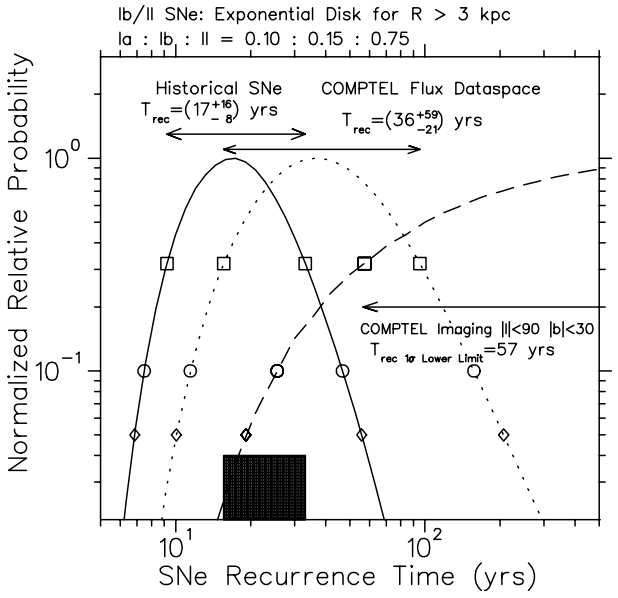


**Fig. B.4.** Normalized relative probability of Galactic SNe rate calculated from three different analysis vs. SNe recurrence time for model **A**. The solid line is the probability of the model in which the number of SNe with $m_V \leq 0$ is 6 in a 1000 year duration. The dashed-line is the probability inferred by maximum likelihood analysis of COMPTEL's 1.157 MeV $\gamma$-line inner galactic ($l \leq 90$, $b \leq 30$) image map. The dotted-line is the relative probability from chi-square test that the 1.157 MeV $\gamma$-line fluxes in the model are consistent with the COMPTEL observed fluxes. The labels of the curves show the optimal, $1\sigma$ ranges, or the $1\sigma$ lower limits of the SNe recurrence time. The boxes, circles, and diamonds on the curves show the $1\sigma$, 90%, and 95% relative probabilities. The shaded area shows the range of the Galactic SNe recurrence time that is consistent with better than $1\sigma$ probability with each of the historical record and the COMPTEL flux dataspace analysis.

2000 yr and assumed that the historical record is 80% complete. A higher SNe rate of 5 SNe per century was obtained by Hatano et al. (1997) who include a population of "ultra-dim" SNe in addition to 4 observed Galactic SNe having $V < 0$ and 80% completeness within the last millenium.

The map and flux methods of estimating supernova rates based on $\gamma$-ray data appear to be significantly different, but they are statistically consistent with each other for a wide range of supernova rates. The imaging analysis gives a smaller rate than the flux analysis, because the data used in the map analysis do not include the Cas A and GRO J0852-4642 $\gamma$-line detections. However, the probability estimate from the flux analysis is a somewhat coarser estimate because the size of independent FOVs used in determining the probability is not known exactly. Ignoring the spatial information begs the question as to why the two brightest SN are in the outer Galaxy rather than in the inner Galaxy where we expected them.

In the flux dataspace analysis, where we ignore the expected spatial distribution of $^{44}$Ti remnants and consider only the measured flux distribution, we find a most probable supernova rate that is more compatible with standard values (such as the rate inferred by the historical record), even for standard $^{44}$Ti yields. However, the COMPTEL map data indicate a lower SN rate (~1 SN/36 yr) than that suggested by the historical record (~1 SN/17 yr). However model **A** which does not have a supernova event in the inner 3 kpc radius has better agreement between the map analysis and the historical record analysis. This suggests that a model with less concentrated supernova near the Galactic center than the model used here could give a better agreement than we obtained here. Also, an extinction model with smaller extinction toward the Galactic center than Hakkilla et al.'s model could give a better agreement than what we present here.

Based on chemical evolution studies, Timmes et al. (1996) estimated that only ~1/3 of the solar $^{44}$Ca abundance is accounted for. Models with a SN rate of ~3 SNe per century and standard $^{44}$Ti yields fail to produce the solar $^{44}$Ca abundance. This rate, when confronted with the gamma-ray data (dashed line in Figs. B.4 and B.5) is too large: the COMPTEL gamma-ray data worsen an already serious problem. Timmes et al. (1996) suggest 3 possibilities:

1. increase the $^{44}$Ti yields by a factor of ~3;
2. increase the supernova rate by a factor of ~3;
3. there is another source of $^{44}$Ca in the Galaxy.

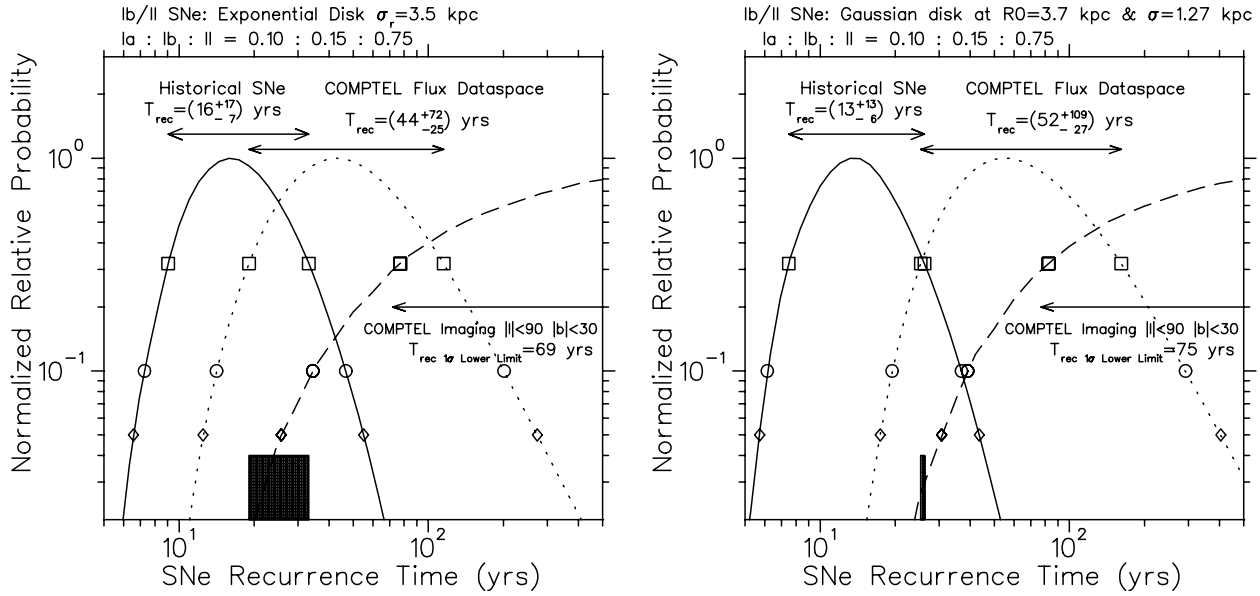


**Fig. B.5.** Same as Fig. B.4 but for models **B** (*left*) and **C** (*right*).

Our analysis in Figs. B.4, and B.5 shows that the first and second option are not compatible with COMPTEL's $^{44}$Ti $\gamma$-line map, which would be brighter by a factor of 3 or exhibit a larger number of $^{44}$Ti hot spots than actually observed. We are thus left with the third option, to seriously entertain the idea that there exists some rare type of supernova (i.e., detonation of helium white dwarf), not realized in recent centuries, that produces very large amounts of $^{44}$Ti.

## Appendix C: Solar $^{44}$Ca constraints

We now wish to estimate the effects of choices of chemical evolution model parameters on the $^{44}$Ca constraint. We do this with analytic models (Clayton 1985). Leising & Share (1994) used that chemical evolution model to estimate the current $^{44}$Ca production rate by requiring the yield that gave exactly the solar abundance 4.55 Gyr ago. With model parameters $k$ (infall contribution) and $\Delta$ (time delay) defining the shape of the galactic infall history, the current production is

$$p(^{44}\mathrm{Ca}) = X_\odot(^{44}\mathrm{Ca})\,\frac{k+1}{\Delta}\,M_\mathrm{g}(T_\mathrm{G}) \times\left[\frac{T_\odot+\Delta}{\Delta}-\left(\frac{T_\odot+\Delta}{\Delta}\right)^{-k}\right]^{-1}, \quad \text{(C.1)}$$

where $T_\mathrm{G}$ is the age of the Galaxy, $T_\odot = T_\mathrm{G} - 4.55$ Gyr, and $M_\mathrm{g}(T_\mathrm{G})$ is mass of interstellar gas participating in star formation now. In this formulation, the $^{44}$Ca production depends mainly on the infall parameter $k = [f(t)/M_\mathrm{G}(t)](t+\Delta)$ and the gas mass, and weakly on $\Delta$ and the age of the Galaxy. The closed-box model, $k = 0$, is ruled out by observations, and $k = 2$–4 is favored from a number of considerations (Clayton et al. 1993). For the total $^{44}$Ca production rate, therefore, a low extreme value of $p(^{44}\mathrm{Ca}) = 1.1\times10^{-6}\ M_\odot\ \mathrm{yr}^{-1}$ is obtained for $k = 1$, $\Delta = 1.0$ Gyr, $M_\mathrm{G}(T_\mathrm{G}) = 4\times10^9\ M_\odot$ , and $T_\mathrm{G} = 13$ Gyr. An upper limit is estimated as $p(^{44}\mathrm{Ca}) = 1.2\times10^{-5}\ M_\odot\ \mathrm{yr}^{-1}$ for $k = 4$, $\Delta = 0.1$ Gyr, $M_\mathrm{G}(T_\mathrm{G}) = 1\times10^{10}\ M_\odot$ , and $T_\mathrm{G} = 10$ Gyr. Our favored value is $p(^{44}\mathrm{Ca}) = 5.5\times10^{-6}\ M_\odot\ \mathrm{yr}^{-1}$, derived for $k = 2$, $\Delta = 0.1$ Gyr, $M_\mathrm{G}(T_\mathrm{G}) = 1\times10^{10}\ M_\odot$ , and $T_\mathrm{G} = 12$ Gyr. As in previous such studies (e.g. Leising & Share 1994) we assume that this equals the $^{44}$Ti production rate. (However, we note the statement by Timmes et al. (1996) that one-half of $^{44}$Ca is made directly as $^{44}$Ca rather than as $^{44}$Ti.) In such models, the solar $^{44}$Ca abundance thus could be provided by, for example, 2.8 SNe per century at the present epoch ejecting on average $2\times10^{-4}\ M_\odot$ of $^{44}$Ti.

## Appendix D: Presolar grains

Do the presolar SiC grains (Clayton & Nittler 2004) that condensed within the expanding supernova interior (Amari & Zinner 1997; Clayton et al. 1997a) shed light on the $^{44}$Ti origin? Called "X grains", each represents a sample of selected portions of a supernova interior, but "what supernova" and "what portions of it" are unidentified questions for each X grain. Deneault et al. (2003) present a physical condensation argument to identify the region within the supernovae; but their argument awaits digestion by the condensation-chemist community. The X grains certainly contain evidence of having condensed with abundant live $^{44}$Ti in the form of very large $^{44}$Ca/$^{40}$Ca ratios (Nittler et al. 1996; Clayton et al. 1997a; Hoppe et al. 2000) that can be explained only through the action of live $^{44}$Ti. This proves their supernova origin, and was a predicted signature of supernova origin for presolar grains (Clayton 1975) from the beginning. If each grain contains sufficient Ca and Ti the SIMS analysis can yield the $^{44}$Ti/$^{48}$Ti abundance ratio at the time of condensation (Fig. 2 of Clayton et al. (1997a) and Figs. 8 and 9 of Hoppe et al. 2000). Many X grains having $^{44}$Ti/$^{48}$Ti = 0.1–0.6 are found. The production ratio required by the assumption that all $^{44}$Ca within solar abundances is the product of decay of $^{44}$Ti is $P(^{44}\mathrm{Ti})/P(^{48}\mathrm{Ti}) = 0.72$; therefore, supernova X grains are found with ratios up to the required bulk production consistent with that assumption.

Despite this it must be clearly understood that the measured production ratio $P(^{44}\mathrm{Ti})/P(^{48}\mathrm{Ti})$ within material in a specific grain bears no simple relationship to the bulk production ratio in the supernova within which that grain condensed. This illustrates the problem of not knowing precisely what supernova material the grain's isotopes reflect. However, this problem seems capable of eventual solution (Deneault et al. 2003).

### *D.1. SNII X grains*

The SiC X grains probably originated in core-collapse SNII. Within them the pure alpha-rich freezeout (Woosley et al. 1973, Sect. VII), which produces the bulk of $^{44}$Ti ejected from SNII, has production ratio near $P(^{44}\mathrm{Ti})/P(^{48}\mathrm{Ti}) = 1$–$2$ (see Fig. 23 of Woosley et al. 1973; The et al. 1998, Sect. 3); so no X grain is pure alpha-rich freezeout material, although some of them must contain a significant fraction of their Ti from the alpha-rich freezeout. On the other hand, the production ratio during normal silicon burning is very much smaller, near $P(^{44}\mathrm{Ti})/P(^{48}\mathrm{Ti}) = 0.01$ (Woosley et al. 1973, Fig. 19). Therefore, X grains having $^{44}$Ti/$^{48}$Ti near 0.01 or less may contain no alpha-rich freezeout material at all, but instead condense from Si-burning ejecta rich in $^{28}$Si.

In their study of 99 SiC X grains from the Murchison meteorite, Hoppe et al. (2000) found that 25 contained enough Ti and Ca for isotopic analysis with the CAMECA IMS3f ion microprobe in Bern. Now that the new nano-SIMS ion microprobe is functional, we may hope for even more complete future surveys with its higher sensitivity. Of the 25 having enough Ti and Ca, 5 revealed large and easily resolved $^{44}$Ca excesses, corresponding to $P(^{44}\mathrm{Ti})/P(^{48}\mathrm{Ti}) > 0.01$. Although the chemistry of condensation of SiC in supernovae has not been solved, initial studies (Deneault et al. 2003) of the location of C and Si suggest that no more than 20% of SiC X grains should be expected to contain $P(^{44}\mathrm{Ti})/P(^{48}\mathrm{Ti})$ ratios in excess of those available during normal O and Si burning. That is, a majority of the X grains should contain no alpha-rich matter even if each supernova ejects such matter. If this be taken as so, the data suggest that the parent supernova population responsible for the 100s of X grains that have been studied did eject alpha-rich freezeout material in addition to its Si-burning matter. If ejection of alpha-rich freezeout matter were instead rare, we expect that the number of SiC grains having large $P(^{44}\mathrm{Ti})/P(^{48}\mathrm{Ti})$ ratios would be significantly less than 20%. Without more detailed understanding of the origin of the X grains it seems plausible to take their evidence to suggest that all SNII eject alpha-rich-freezeout matter.

If the SiC X grains do originate in SNII, their frequent $^{44}$Ca excesses demonstrate that either the X grains all originated in a single nearly supernova that did eject $^{44}$Ti or originated in many presolar SNII that mostly ejected $^{44}$Ti (although not necessarily always). The properties of the "mainstream SiC grains" enable us to argue against the possibility of a single supernova as origin of the X grains. The much more abundant mainstream grains, which are thought to have originated in presolar carbon stars, have been argued on the basis of their Si isotopes to have been the result of a great many C stars. Their Si isotopic compositions represent approximately the initial Si isotopic compositions from which the intermediate-mass stars formed, and their correlation between excess $^{29}$Si and $^{30}$Si is explained by galactic chemical evolution effects that have produced a wide range of Si isotopic compositions in a large number of C stars (Timmes & Clayton 1996; Clayton 2003). Because the mainstream grains comprise about $10^{-4}$ of all interstellar Si, much of which is quite old, and because the condensed SiC from the C-star phase is but a small fraction of all Si ejected from stars, it seems that the lifetime of SiC grains in the ISM is not short. If this be so, the lifetime of X SiC grains is also not short, suggesting a substantial number of contributing supernovae to the matter gathered into any cloud in the ISM.

### *D.2. SNIa X grains*

For the question of $^{44}$Ti gamma-ray hotspots the issue arises whether the SiC X grains may instead have arisen from exploding SNIa. After all, the high expectation for seeing $^{44}$Ti supernova remnants shown in Fig. 1 came from the assumption that type II are the sources of $^{44}$Ti nucleosynthesis and therefore also of the solar $^{44}$Ca abundance. The absence of such sources could be explained if rare type I events produced much larger yields than are expected from type II. Do the supernova grains offer any guidance? Clayton et al. (1997b) showed that isotopically good fits to X grains might originate within He caps on exploding C,O white dwarfs. Huge production ratios, up to $P(^{44}\mathrm{Ti})/P(^{48}\mathrm{Ti}) = 100$, occur in those He shell zones having peak $T_9 > 1$ (see their Fig. 6). These are too great for existing observations of X grains, suggesting that SNIa are not their sources. However, Clayton et al. (1997b) showed that good fits to all isotopes require that the He caps undergo considerable post-explosive mixing prior to condensation of the X grains. Their Table 2 shows production ratios as small as 0.01 in an average of zones 1–8 (the coolest eight zones) and near 10 in an average over all sixteen zones. (The reader must note that much $^{48}$Ti production is listed by them under $^{48}$Cr, its radioactive progenitor.) The isotopic possibility must therefore be addressed that the $^{44}$Ti-rich X grains are from SNIa He caps rather than from SNII. The discovery of even a single X-type SiC grain containing an initial ratio $^{44}$Ti/$^{48}$Ti = 5 or greater would demonstrate that the He-cap SNIa do exist and that they can condense SiC. This would amount to an existence proof for these rare $^{44}$Ti producers. But no such grain has yet been detected.

Clayton et al. (1997b) pointed out that if the SNIa are near the Chandrasekhar mass, the He cap can be no more than 0.01 $M_\odot$ so that less than $10^{-5}$ $M_\odot$ of $^{44}$Ti is ejected. Such events would be both rare and dim in $^{44}$Ti lines. However, a much larger He cap is involved if the white dwarf is sub-Chandrasekhar (larger) and the detonation begins in a massive He cap. Large amounts of $^{44}$Ti are ejected from such models (Woosley & Weaver 1994), so that the rates of such events are limited by the requirement that they not overproduce the galactic $^{44}$Ca abundance. If this occurs, the rarity of these events in time could account for their absence in the COMPTEL data (see also the Discussion). The relevance of the X grains derives

from the physical unlikelihood of condensation of X grains in such He caps. Their expansion is very fast, and the radiation environment intense, so that even the formation of molecules seems unlikely until the density has become too low for the growth of a 1-micrometer grain of SiC. Clayton et al. (1997b) note that even the possibility of grain condensation would seem to require 3-D explosive modeling in order that some of the He cap can remain at low velocity ("slow He"). This entire problem will require more study before plausibility of SiC X grains from SNIa can be admitted. We therefore conclude that the $^{44}$Ti-bearing X grains have arisen in SNII.

### *D.3. ISM Inhomogeneity of $^{44}$Ca from He-cap SNIa*

We turn now to non-supernova Stardust whose $^{44}$Ca ratios reflect the initial compositions of their donor stars. The supernova X grains seem to support the assumptions that led to the conflict between the COMPTEL map (Fig. 1) and the expected hotspots (Fig. 2); namely, that X grains condensed within SNII, that the number of contributing SNII was large, and that most ejected alpha-rich freezeout matter. However, X grains do not demonstrate that the bulk ejecta of SNII contain sufficient mass of $^{44}$Ti to account for the natural $^{44}$Ca abundance. To test for the presence of rare large $^{44}$Ti producers (Woosley & Weaver 1994) responsible for making good the shortfall from SNII we turn to the mainstream SiC grains with the following original argument. Rare SNIa responsible for roughly 2/3 of galactic $^{44}$Ca plausibly result in Galactic inhomogeneities in the interstellar $^{44}$Ca/$^{40}$Ca ratio that should be larger than those seen by astronomers for elemental-ratio variations attributed to inhomogeneous incorporation of SNII ejecta. It must be slower to homogenize the ISM if SNIa occurring every 3000 yr contribute 2/3 of $^{44}$Ca abundance than for homogenizing ISM from SNII occurring every 30 yr and making but 1/3 of the $^{44}$Ca abundance. ISM regions temporarily enriched in the rare SNIa ejecta may make stars having larger $^{44}$Ca/$^{40}$Ca initial ratios. The mainstream SiC grains reflect the interstellar composition from which the carbon stars formed. That is, factor of two or more variations in $^{44}$Ca/$^{40}$Ca ratio should be present in the initial compositions of stars.

It is this expectation that the mainstream grains may speak against. Hoppe et al. (2000) measured Ca isotopes in 28 mainstream SiC grains (see their Fig. 8) and found their $^{44}$Ca/$^{40}$Ca ratios to be indistinguishable from solar despite large Si isotope variations in the same stars demonstrating that the grains come from different AGB C stars having distinct chemical evolution histories for their initial compositions (Timmes & Clayton 1996). Each mainstream grain was consistent with solar $^{44}$Ca/$^{40}$Ca ratio and their average was enriched 3.8% in $^{44}$Ca, as expected for modest s-process enrichments of AGB atmospheres by the third dredge ups. Because of the small numbers of Ca atoms in mainstream grains, however, individual grain ratios were uncertain by at least 20%. Even so, 20% is a small inhomogeneity for rare events producing 2/3 of the bulk $^{44}$Ca. To improve this data base we call for high precision measurements of the $^{44}$Ca/$^{40}$Ca ratio in a sample of mainstream grains with the new nanoSIMS ion microprobes. Such a survey could reveal more precisely any variations in initial $^{44}$Ca/$^{40}$Ca ratios in intermediate-mass stars expected if the $^{44}$Ti synthesis has instead been the result of a few rare events of very large $^{44}$Ti yield. The present data speak against that. The new arguments that we have presented here can all be improved dramatically in the next few years. Although their message today is not statistically certain, their sense is to support the original conflict that we have displayed in Fig. 2. Because the $^{44}$Ca/$^{40}$Ca ratio in mainstream grains from many AGB stars is very near to the solar ratio, we point out that it is no longer possible to entertain the idea that the sun may itself contain an anomalous $^{44}$Ca/$^{40}$Ca ratio. One can not blame the inability of standard models of the chemical evolution of the galaxy to produce enough $^{44}$Ca by speculating that the sun is abnormally rich in its $^{44}$Ca content.

It should be noted that a thorough study of stardust isotopic inhomogeneity within the context of inhomogeneous galactic chemical evolution has been presented by Nittler (2005). He shows in particular that correlations between Si and Ti isotopic compositions found in stardust can not be accounted for by inhomogeneous GCE. He does not, however, discuss the variations in $^{44}$Ca/$^{40}$Ca that are generated by his model owing to the He-cap SNIa. On the other hand, his calculations may not be ideal for this problem because his model admixes into a homogeneous ISM the same fraction for each supernova's ejecta ($a = 1.7 \times 10^{-5}$) after Monte Carlo sampling to obtain $N = 70$ supernovae. Nonetheless, that paper shows the potential power of stardust to delimit GCE inhomogeneities in general. This approach should be reconsidered carefully when a good data set for initial $^{44}$Ca/$^{40}$Ca in stardust is available.

Mainstream SiC grains are probably not the best grains with which to measure initial stellar $^{44}$Ca/$^{40}$Ca abundance ratios. The mainstream SiC grains contain very little Ca because Ca is much less favored chemically than is Ti within thermally condensing SiC grains. The hibonite Stardust grains described by Nittler et al. (2005), on the other hand, contain much more Ca because Ca is an essential ingredient of the hibonite crystal structure. Therefore, accurate measurements of $^{44}$Ca/$^{40}$C in hibonite grains could reveal better information relevant to ISM inhomogeneity of the $^{44}$Ca/$^{40}$Ca ratio.